

NEGATE: Constrained Semantic Guidance for Linguistic Negation in Text-to-Video Diffusion

Taewon Kang¹, Ming C. Lin^{1*}

¹University of Maryland at College Park, United States

taewon@umd.edu, lin@umd.edu

Abstract

Negation is a fundamental linguistic operator, yet it remains inadequately modeled in diffusion-based generative systems. In this work, we present a formal treatment of linguistic negation in diffusion-based generative models by modeling it as a structured feasibility constraint on semantic guidance within diffusion dynamics. Rather than introducing heuristics or retraining model parameters, we reinterpret classifier-free guidance as defining a semantic update direction and enforce negation by projecting the update onto a convex constraint set derived from linguistic structure. This novel formulation provides a unified framework for handling diverse negation phenomena, including object absence, graded non-inversion semantics, multi-negation composition, and scope-sensitive disambiguation. Our approach is training-free, compatible with pretrained diffusion backbones, and naturally extends from image generation to temporally evolving video trajectories. In addition, we introduce a structured negation-centric benchmark suite that isolates distinct linguistic failure modes in generative systems, to further research in this area. Experiments demonstrate that our method achieves robust negation compliance while preserving visual fidelity and structural coherence, establishing the first unified formulation of linguistic negation in diffusion-based generative models beyond representation-level evaluation.

1. Introduction

Vision-language models (VLMs) have achieved remarkable success in text-conditioned image and video generation. Modern diffusion-based systems can synthesize complex visual scenes from natural language descriptions with high fidelity and compositional richness [7, 45]. However, despite these advances, a fundamental limitation persists: current generative models struggle to correctly interpret and enforce *linguistic negation*. Negation is not merely the ab-

sence of a concept, nor is it equivalent to supplying an externally specified exclusion. Prompts such as “a highway at sunset, with no vehicles,” “a person holding a phone but not using it,” or “a room that is not unlit” encode structured linguistic constraints involving scope, composition, graded moderation, and logical interaction. Psycholinguistic studies suggest that negation is processed through activation followed by inhibition of affirmative representations [21, 22], highlighting its structured and dynamic nature. Existing generative models frequently violate these constraints, producing outputs that include forbidden objects, misapply scope, or over-correct toward unintended opposites. This failure reveals a deeper gap: while diffusion models align with affirmative semantics, they lack a principled formulation for negation as a structured linguistic operator.

Recent work has highlighted this limitation from a representational perspective. In particular, recent work [2, 35, 44] demonstrates that vision-language models often fail to distinguish between positive and negated captions in retrieval settings. These studies establish that negation sensitivity is weak at the embedding level. However, they primarily focus on *benchmarking* representation separability in static image–text matching. They do not address how negation should influence the generative process itself, nor how structured linguistic negation can be enforced over temporal trajectories in video generation.

In this work, we shift the perspective from representation evaluation to *generative formulation*. We ask a different question: how should linguistic negation be modeled as part of the semantic content of a prompt, and how should that modeling constrain the evolution of generative trajectories? Rather than treating negation as a data deficiency to be corrected through retraining, we formalize negation as a structured feasibility condition on semantic guidance within diffusion dynamics, drawing inspiration from constrained dynamical perspectives in diffusion-based control [48, 50]. More specifically, we reinterpret classifier-free guidance as defining a semantic update direction in latent space and treat negation as a constraint restricting projection along di-

*Corresponding author

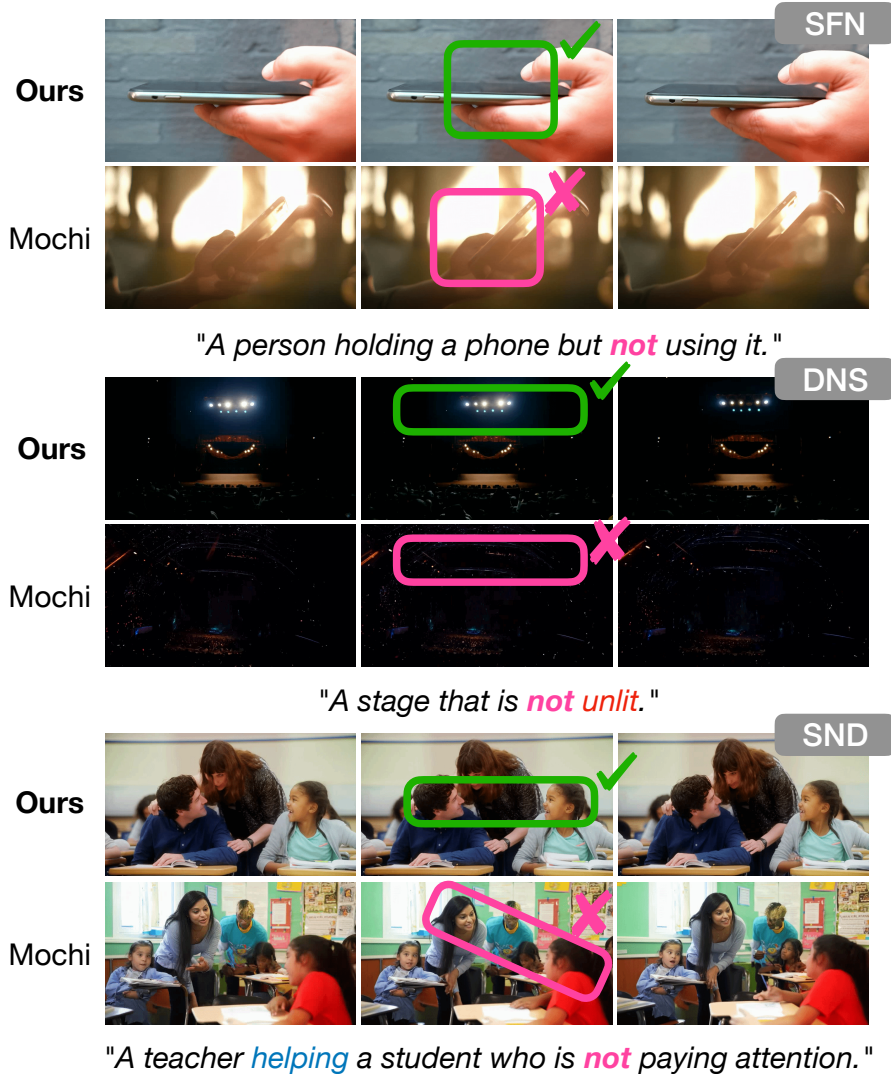


Figure 1. **Negation beyond object removal.** Structural Functional Negation (SFN), Double Negation Sensitivity (DNS), and Scoped Negation Disambiguation (SND). Baseline diffusion models collapse negation into semantic inversion or scope errors, whereas our model enforces negation as a constraint on diffusion dynamics, yielding correct logical interpretation and stable scene composition. Qualitative results and comparisons with more video diffusion models are provided in Section 4.3.

reactions associated with negated concepts. This leads to a convex feasibility formulation in which each diffusion step computes the minimal modification required to restore compliance. Most importantly, this formulation does not introduce a new generative backbone, nor does it require retraining. Instead, it provides a *principled mapping from linguistic structure to constraint geometry in semantic guidance space*.

This modeling perspective enables us to systematically handle diverse linguistic phenomena, including: (i) object-level absence, (ii) temporal suppression in evolving scenes, (iii) implicit category exclusivity, (iv) multi-negation com-

position, (v) structural functional negation, (vi) graded non-inversion semantics, (vii) double negation sensitivity, and (viii) scope-sensitive disambiguation. Although linguistically distinct, we show that all of these cases admit a unified convex constraint parameterization, transforming heterogeneous negation forms into a consistent feasibility problem over generative trajectories. Notably, our formulation extends beyond static image generation. Because constraints are enforced at the level of trajectory evolution, the framework naturally applies to video generation, where negation violations may emerge temporally after initial structure formation. More broadly, the approach generalizes to *vision-*

language-action (VLA) settings, where language may constrain not only visual content but also dynamic behavior. We further introduce a structured negation-centric benchmark suite designed to isolate and evaluate distinct linguistic failure modes in generative systems. Unlike prior negation datasets focused on representation separability [2, 35], our benchmark measures distributional compliance under structured constraints, explicitly targeting trajectory-level violations.

The key contributions of this work are threefold:

- 1. Formal Modeling of Linguistic Negation in VLMs.** We provide the first unified formulation that models diverse linguistic negation phenomena as *structured convex feasibility constraints in semantic guidance space*.
- 2. Constraint-Based Generative Enforcement.** We introduce a training-free mechanism that enforces negation during diffusion through minimal-energy projection, ensuring stability and compliance without architectural modification.
- 3. Structured Benchmarking Beyond Representation.** We construct a *negation-centric evaluation suite spanning eight linguistically distinct categories*, enabling systematic assessment of generative compliance in both image and video settings.

By reframing negation as a structured semantic constraint rather than a prompt heuristic or embedding deficiency, this work bridges linguistic theory and generative modeling. It establishes a principled foundation for constraint-consistent vision-language generation, moving beyond surface-level prompt alignment toward linguistically grounded generative control.

2. Related Work

2.1. Negation and Compositionality in Vision-Language Models

Negation is a fundamental yet challenging phenomenon in language understanding. Psychological studies suggest that negation is processed through a two-stage mechanism in which the affirmative representation is first activated and subsequently inhibited [21, 22]. This cognitive perspective highlights that negation is not merely the absence of affirmation, but an active semantic operation. Compositional weaknesses in modern vision-language models (VLMs) were exposed by Winoground [36], which revealed near-chance performance when matching captions containing identical words in different orders. The ARO benchmark [47] showed that many VLMs behave like bag-of-words models, largely ignoring relational and order structure, while SugarCrepe [20] identified exploitable biases in compositional benchmarks. Building on these findings, Learn “No” to Say “Yes” Better [35], NegBench [2], and NegVQA [52] demonstrated significant degradation

under negated queries across retrieval and VQA settings, and CLIPGLASSES [44] improved negation sensitivity via inference-time embedding adjustments. These efforts operate at the representation level and primarily address alignment deficiencies. In contrast, our approach does not alter representation learning. Instead, we *formulate linguistic negation as a dynamical feasibility constraint that directly governs diffusion guidance updates* during sampling.

2.2. Inference-Time Control and Constrained Diffusion

Inference-time intervention has become central to semantic control in diffusion models [3, 5, 6, 8–10, 15–18, 23, 24, 27–31, 33, 34, 37–43, 46, 49, 51], including text-to-video systems such as Imagen Video [19] and Make-A-Video [34]. Training-free compositional methods manipulate cross-attention [11], combine energy components [26], or align syntax-aware attention maps [32]. Concept editing approaches, including Erasing Concepts from Diffusion Models [13] and Unified Concept Editing [14], modify model weights—often via closed-form projections—to permanently remove or alter concepts. Constrained sampling has been explored via projection or proximal updates [48, 50], and broader probabilistic frameworks such as Posterior Regularization [12] impose structured constraints during model learning. LLM-grounded Video Diffusion [25] further injects structured language planning into video generation. While these approaches manipulate attention, combine energies, edit weights, or enforce spatial and latent constraints, negation is treated implicitly as a conditioning or suppression signal rather than as a logically defined constraint over generative dynamics. Our formulation differs in that we *derive a closed-form minimal correction satisfying a half-space feasibility condition in semantic guidance space*. Rather than heuristically amplifying or suppressing tokens, we *compute the smallest admissible update required to enforce negation consistency* at each timestep. Furthermore, unlike classical control formulations defined over physical states [4], we *operate in semantic guidance space and derive analytic projections tailored to linguistic negation*. This enables a principled treatment of negation across both image and video diffusion backbones without retraining or architectural modification.

3. Method

We formulate linguistic negation in vision-language generation as a feasibility constraint imposed on semantic guidance within pretrained diffusion dynamics. Rather than introducing explicit repulsive potentials or heuristic gradient subtraction, we compute at each timestep the minimal correction to a reference semantic guidance update required to satisfy a negation-consistent convex constraint.

Our formulation separates three components: (i) pre-

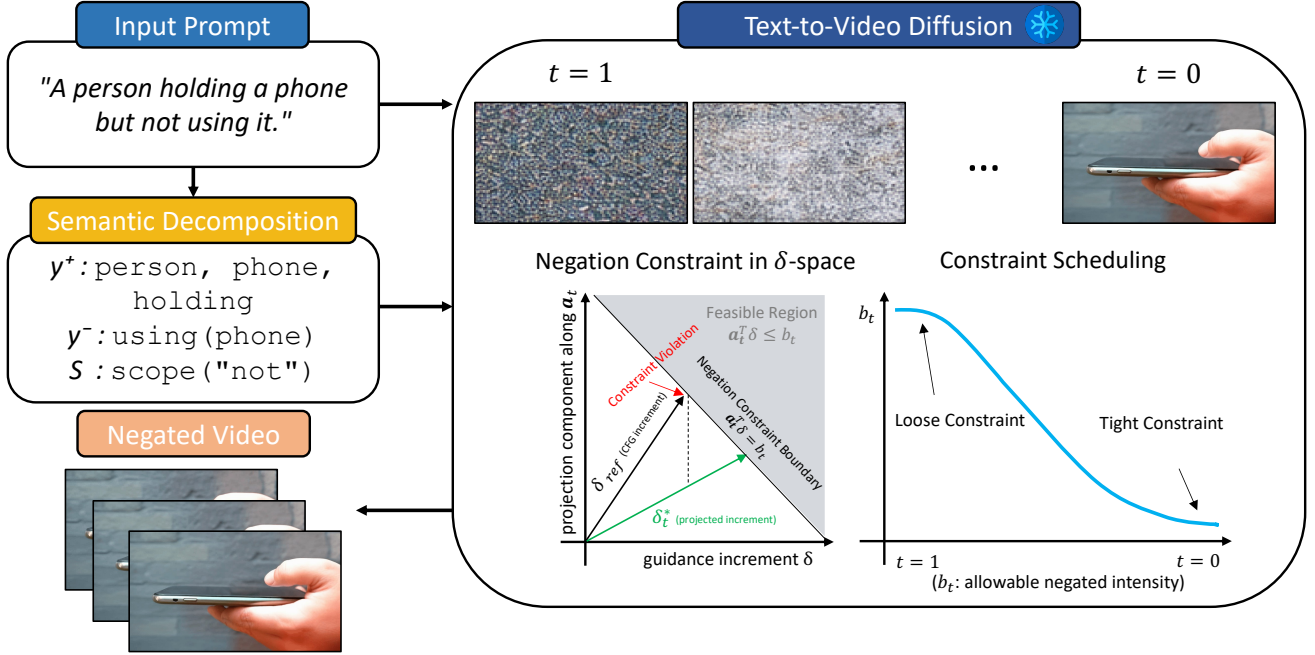


Figure 2. **Overview of our negation-aware framework via convex feasibility projection.** Given a natural-language prompt containing linguistic negation (e.g., “a person holding a phone but not using it”), we first perform *semantic decomposition* into affirmed concepts y^+ , negated concepts y^- , and scope structure \mathcal{S} . In classifier-free guidance (CFG), the reference guidance increment is defined as $\delta_{\text{ref}} = \gamma(\epsilon_{\text{text}} - \epsilon_{\text{uncond}})$, which attracts the diffusion trajectory toward affirmed semantics but does not constrain negated variables. We construct a negation direction $a_t = \epsilon_{\text{neg}} - \epsilon_{\text{uncond}}$, representing the semantic increment that increases alignment with the negated concept. At each reverse-time step ($t = 1 \rightarrow 0$), we enforce a half-space constraint $a_t^\top \delta \leq b_t$ in guidance space and project the reference increment onto the feasible region, producing the corrected update δ_t^* . A temporal scheduling strategy progressively tightens the constraint threshold b_t , allowing early structural formation while enforcing strict negation at later stages. The resulting denoising trajectory yields negation-compliant video generation without retraining the text-to-video diffusion model.

trained diffusion dynamics, (ii) semantic guidance directions induced by language, and (iii) a feasibility operator derived from linguistic negation structure.

3.1. Controlled Diffusion Dynamics

Let $x_t \in \mathbb{R}^{N \times d}$ denote the latent variable at diffusion time $t \in [0, 1]$, where $t = 1$ corresponds to pure Gaussian noise and $t = 0$ corresponds to the data sample. Sampling proceeds by integrating the reverse-time probability flow ODE

$$\frac{dx_t}{dt} = f_\theta(x_t, t), \quad (1)$$

from $t = 1$ to $t = 0$, where f_θ is a fixed pretrained diffusion backbone.

The diffusion network is trained to predict the additive Gaussian noise injected during forward diffusion. We denote this prediction by

$$\epsilon_\theta(x_t, t, c),$$

where c is a conditioning embedding.

Let $\Phi(\cdot)$ denote the pretrained text encoder. Given a prompt y , its conditioning embedding is defined as

$$c = \Phi(y).$$

Classifier-free guidance (CFG) modifies the predicted noise as

$$\epsilon_{\text{CFG}} = \epsilon_{\text{uncond}} + \gamma(\epsilon_{\text{text}} - \epsilon_{\text{uncond}}), \quad (2)$$

where

$$\epsilon_{\text{text}} = \epsilon_\theta(x_t, t, c), \quad \epsilon_{\text{uncond}} = \epsilon_\theta(x_t, t, \emptyset),$$

and $\gamma > 0$ is the guidance scale.

We define the reference semantic increment

$$\delta_{\text{ref}} = \gamma(\epsilon_{\text{text}} - \epsilon_{\text{uncond}}), \quad (3)$$

which represents the semantic guidance direction that increases alignment with affirmed semantics. However, this reference increment does not explicitly constrain negated concepts.

3.2. Semantic Decomposition of Linguistic Negation

Given a prompt y , we decompose it into

$$y = (y^+, y^-, \mathcal{S}),$$

where:

- y^+ encodes affirmed semantic components,
- y^- encodes the linguistically grounded semantic span subject to negation or restriction,
- \mathcal{S} encodes syntactic scope and logical composition structure.

This decomposition is obtained through a deterministic linguistic preprocessing stage operating at the span and predicate level. We identify negation operators or restrictive modifiers (e.g., explicit negation cues, *only*-constraints, contrastive conjunctions, and logical modifiers) and extract the minimal syntactic unit governed by each operator using dependency structure. Depending on linguistic form, the extracted unit may correspond to: (i) an object-level noun phrase (e.g., absent object), (ii) a predicate or action phrase (functional negation), (iii) a category-level restriction (implicit allow-set constraints), (iv) a temporally modulated clause, or (v) a logically composed span involving multiple operators. Rather than enumerating object instances or rewriting prompts, we canonicalize the extracted span into a semantically coherent phrase suitable for encoding. For restrictive forms such as “only X,” the allow-set is interpreted as inducing a complementary semantic direction at the category level. For functional negation, predicate structure is preserved. For nested or multiple negations, \mathcal{S} retains compositional information so that logical sign or sequential constraints can be consistently parameterized downstream.

Let

$$c_{\text{neg}} = \Phi(y^-)$$

denote the conditioning embedding obtained by applying the same pretrained text encoder to the isolated negated component.

A negation branch is constructed as

$$a_t = \epsilon_{\text{neg}} - \epsilon_{\text{uncond}}, \quad (4)$$

where

$$\epsilon_{\text{neg}} = \epsilon_{\theta}(x_t, t, c_{\text{neg}}).$$

All noise predictions are obtained from the same pretrained diffusion model $\epsilon_{\theta}(\cdot)$ without additional training. The resulting vector a_t represents the local semantic direction that increases alignment with the extracted negated span under the current latent state. Importantly, a_t does not correspond to an antonymic or manually inverted direction. Instead, it captures the intrinsic diffusion direction associated with the linguistic unit identified as restricted. Linguistic negation is therefore enforced by constraining mo-

tion along a_t , rather than replacing the concept with its opposite or introducing external heuristic penalties. This formulation ensures that diverse negation phenomena—object absence, functional suppression, category restriction, logical composition, temporal modulation, and scope disambiguation—are uniformly reduced to structured span extraction followed by convex feasibility enforcement in semantic guidance space.

3.3. Negation as Convex Feasibility

We interpret linguistic negation as restricting semantic projection along a_t . Define

$$\phi_t(\delta) = a_t^\top \delta. \quad (5)$$

Negation is enforced by requiring

$$\phi_t(\delta_t) \leq b_t. \quad (6)$$

This defines a closed half-space in guidance space. The bound b_t determines the admissible semantic intensity of the negated concept. Different linguistic forms correspond to different constraint parameterizations:

$$\text{Absent Object Consistency (AOC): } b_t \leq 0 \quad (7)$$

$$\text{Non-Inversion Mitigation (NMI): } b_t = \tau_t \quad (8)$$

$$\text{Double Negation Sensitivity (DNS): } a_t \leftarrow \sigma_t a_t \quad (9)$$

$$\text{Scoped Negation Disambiguation (SND): } a_t = a_{t,i^*} \quad (10)$$

where $\sigma_t \in \{-1, 1\}$ encodes logical composition and i^* is determined by syntactic structure. Thus diverse linguistic phenomena reduce to a unified convex constraint on semantic projection.

3.4. Minimal-Energy Projection

We compute the corrected update via

$$\delta_t^* = \arg \min_{\delta} \frac{1}{2} \|\delta - \delta_{\text{ref}}\|_2^2 \quad \text{s.t.} \quad a_t^\top \delta \leq b_t. \quad (11)$$

The Karush–Kuhn–Tucker (KKT) conditions yield:

$$\delta_t^* = \delta_{\text{ref}} - \lambda_t a_t, \quad (12)$$

with

$$\lambda_t = \frac{\max\{0, a_t^\top \delta_{\text{ref}} - b_t\}}{\|a_t\|_2^2}. \quad (13)$$

Thus projection occurs only when feasibility is violated. The final prediction becomes

$$\epsilon_t^* = \epsilon_{\text{uncond}} + \delta_t^*. \quad (14)$$

3.5. Stability and Convergence Properties

Because the feasible set is convex and the objective is strictly convex, the solution exists and is unique.

Furthermore, projection onto a closed half-space is non-expansive:

$$\|\delta_t^* - \delta_t'^*\| \leq \|\delta_{\text{ref}} - \delta_{\text{ref}}'\|. \quad (15)$$

This ensures Lipschitz continuity of the corrected guidance.

Unlike steep repulsive potentials, the projection does not introduce stiffness into the ODE. The correction magnitude is bounded by

$$\|\delta_t^* - \delta_{\text{ref}}\| = \lambda_t \|a_t\| \leq \frac{|a_t^\top \delta_{\text{ref}} - b_t|}{\|a_t\|}. \quad (16)$$

Thus no oscillatory amplification occurs.

3.6. Temporal Scheduling

We define

$$b_t = (1 - \alpha_t)b_{\text{init}} + \alpha_t b_{\text{final}}, \quad (17)$$

with

$$\alpha_t = \left(\frac{t}{T}\right)^p. \quad (18)$$

Early diffusion emphasizes structural formation (b_t loose), while later stages enforce strict compliance.

3.7. Unified Treatment of Linguistic Cases

The category-specific parameterizations below operate on (a_t, b_t) constructed from the parsed negated span y^- and its scope \mathcal{S} . Importantly, a_t is always computed from the same pretrained diffusion backbone via $c_{\text{neg}} = \Phi(y^-)$; therefore, diversity across linguistic phenomena arises from structured span extraction rather than model modification. We explicitly parameterize linguistic negation across eight structured categories, which will later form our benchmarking suite:

- Absent Object Consistency (AOC)
- Late Emergence Negation (LEN)
- Implicit Natural-Only Attribute (INA)
- Multi-Negation Composition (MNC)
- Structural Functional Negation (SFN)
- Non-Inversion Mitigation (NMI)
- Double Negation Sensitivity (DNS)
- Scoped Negation Disambiguation (SND)

Each category corresponds to a distinct linguistic phenomenon but can be represented through the same convex feasibility structure by appropriate parameterization of (a_t, b_t) :

$$\text{AOC: } b_t \leq 0 \quad (\text{strict absence}) \quad (19)$$

$$\text{LEN: } b_t = b_t(t) \quad (\text{time-varying bound}) \quad (20)$$

$$\text{INA: } a_t \in \text{complement category space} \quad (21)$$

$$\text{MNC: } \text{sequential half-space projections} \quad (22)$$

$$\text{SFN: } a_t = \nabla(\text{functional attribute}) \quad (23)$$

$$\text{NMI: } b_t = \tau_t > 0 \quad (\text{bounded moderation}) \quad (24)$$

$$\text{DNS: } a_t \leftarrow \sigma a_t \quad (\text{logical sign composition}) \quad (25)$$

$$\text{SND: } a_t = a_{t,i^*} \quad (\text{scope-resolved direction}) \quad (26)$$

Thus, although linguistically diverse, all eight negation categories reduce to convex feasibility enforcement in semantic guidance space. This unified treatment clarifies that the contribution lies not in inventing a new diffusion controller, but in formally modeling linguistic negation structure and demonstrating that diverse corner cases admit a principled projection-based solution.

4. Experiments and Results

4.1. Implementation Details

Our method is implemented as a constraint-aware guidance formulation within diffusion sampling, without modifying or retraining the backbone model. During classifier-free guidance, we compute three prediction branches: unconditional, affirmative text-conditioned, and a negation-conditioned branch derived from the input prompt. Instead of directly subtracting the negation prediction, we interpret negation as a soft inequality constraint on the guidance direction and perform a minimal-energy projection of the attractive CFG update onto a time-dependent half-space defined by the negation branch. The constraint strength follows a polynomial schedule $\alpha_t = (t/T)^p$ with $p = 2.0$, gradually tightening semantic suppression toward later timesteps. The final bound on the negation-direction component is set to 0.0, enforcing asymptotic removal of the forbidden concept, and numerical stabilization uses $\varepsilon = 10^{-8}$. The initial constraint bound is determined from the first-step inner product per sample and annealed thereafter. All backbone-specific parameters (e.g., inference steps, scheduler, guidance scale) follow default configurations [1], and no additional learnable parameters are introduced.

4.2. Benchmarking Datasets

Standard vision-language benchmarks are **insufficient for evaluating generative negation compliance**. Existing datasets such as MS-COCO, WebVid, or negation-focused retrieval benchmarks are designed to measure representation separability or caption alignment, rather than distributional behavior of generated samples under negation constraints. Negation prompts are rare and not systematically

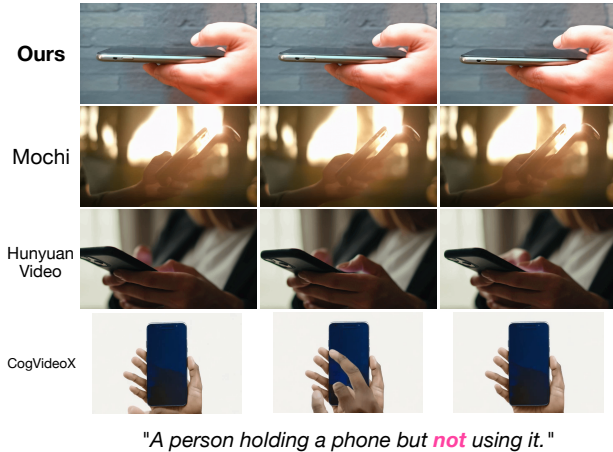


Figure 3. **Representative qualitative comparison (SFN).** We compare our model with state-of-the-art diffusion baselines (Mochi, HunyuanVideo, CogVideoX) on Structural Functional Negation (SFN): “A person holding a phone but not using it.” While baselines often collapse the negation into unintended interaction (e.g., phone-using gestures) or fail to maintain the intended constraint, our model preserves the object presence and suppresses the prohibited behavior, demonstrating negation control beyond object removal.

structured, and these datasets do not capture temporal emergence of forbidden concepts in video diffusion. To address this gap, we construct a controlled negation-centric evaluation suite specifically designed to probe constraint enforcement during generation. The benchmark consists of eight complementary categories targeting distinct linguistic and dynamical failure modes. All quantitative results in the main paper are averaged over this benchmark. Rather than maximizing prompt volume, our benchmark prioritizes linguistic precision and categorical coverage, with each prompt carefully designed to isolate the target negation phenomenon and prevent confounding across adjacent linguistic categories. The dataset is used exclusively for evaluation; no training or fine-tuning is performed. **Detailed dataset construction, category definitions, and examples are provided in Appendix B.**

4.3. Qualitative Results

Figure 3 shows a representative comparison on Structural Functional Negation (SFN), where the target object must remain present while a prohibited interaction is suppressed (“a person holding a phone but not using it”). This setting is particularly challenging because negation cannot be satisfied by simply removing the object; instead, it requires behavior-level control while preserving the overall scene structure. State-of-the-art diffusion baselines frequently produce unintended phone-using gestures or fail to maintain the negated constraint consistently. In contrast, our

model enforces negation as a constraint on diffusion dynamics, preserving object presence and scene composition while suppressing the forbidden semantics. **More qualitative results across diverse negation categories and additional model comparisons are provided in Appendix C.**

4.4. Quantitative Evaluation

We evaluate negation-aware generation using standard, widely adopted metrics without modifying prompts or introducing threshold-based rules. Our evaluation measures (1) global prompt alignment, (2) negated concept suppression, and (3) object-level presence. Global alignment is measured using CLIPScore between generated frames and the full textual prompt, including negation phrases. Negation compliance is quantified via CLIP similarity to the explicitly negated concept (CLIP-neg), where lower values indicate stronger suppression. We further compute BLIP-based caption similarity for text-level semantic fidelity and open-vocabulary detection confidence (DINO-conf) for object-level presence of the forbidden concept. To complement embedding-based evaluation, we additionally introduce two direct vision-language metrics: the *Negation Compliance Score (NCS)* and the *Negation Violation Rate (NVR)*. NCS is obtained from a multimodal language model that directly reasons over sampled video frames and assigns a 1–5 compliance score, while NVR measures the empirical frequency of explicit forbidden-concept violations under the same judge. These metrics evaluate negation satisfaction at the semantic reasoning level rather than within embedding space. Detailed definitions and implementation details are provided in the Supplementary. All results are averaged over our structured benchmark. As shown in Table 1, our method achieves the highest CLIPScore while simultaneously reducing CLIP-neg and DINO-conf compared to baselines. Importantly, it also attains the highest NCS and the lowest NVR, confirming improved negation compliance under direct multimodal reasoning. Notably, negation-aware control improves both global alignment and constraint compliance, demonstrating that trajectory-level constraint enforcement does not degrade positive semantic fidelity. **More quantitative analysis are provided in Appendix D.**

4.5. Ablation Study

We ablate our two core components: (i) the repulsive constraint term and (ii) time-dependent constraint scheduling. The repulsive term determines *what* semantic direction is suppressed, while scheduling controls *when* suppression is enforced along the diffusion trajectory. As shown in Table 1, removing the repulsive term restores CLIP-neg to near-baseline levels and increases object-level detection confidence, while leaving global CLIPScore largely unchanged. This confirms that negation compli-

Method	CLIPScore \uparrow	CLIP-neg \downarrow	BLIP \uparrow	DINO-conf \downarrow	NCS \uparrow	NVR \downarrow
Mochi	0.2857	0.2411	0.8183	0.0175	3.5789	0.3625
HunyuanVideo	0.2743	0.2620	0.7776	0.0184	3.4584	0.3675
CogVideoX	0.2836	0.2442	0.7869	0.0181	3.4080	0.3800
Ours (Full Model)	0.2924	0.2336	0.8201	0.0167	4.0700	0.2300
Ours w/o Repulsive Energy	0.2924	0.2411	0.8128	0.0181	3.9548	0.2625
Ours w/o Constraint Scheduling	0.2800	0.2405	0.7869	0.0174	3.5789	0.3625

Table 1. **Quantitative evaluation of negation-aware video generation.** CLIPScore measures overall alignment between generated frames and the full textual prompt. CLIP-neg reports similarity between generated frames and the negated concept (lower is better). BLIP evaluates caption-level semantic alignment without modifying the prompt. DINO-conf denotes the average detection confidence of negated objects (lower indicates stronger negation compliance). Refer Appendix D for detailed analysis.

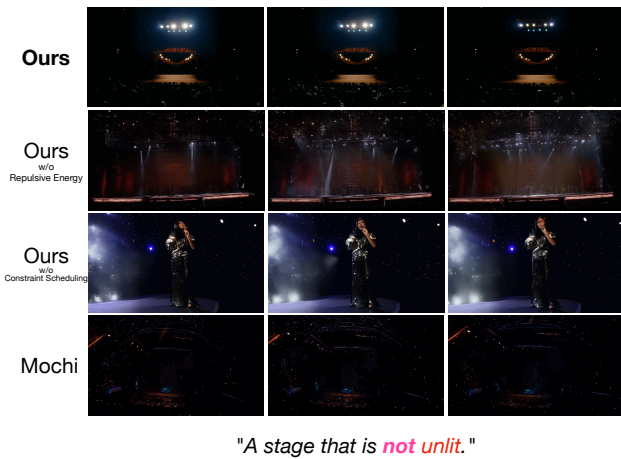


Figure 4. **Ablation study on negation control.** We compare the our full model with two ablations—*w/o Repulsive Energy* and *w/o Constraint Scheduling*—and a strong diffusion baseline (Mochi) on a double-negation prompt (DNS): “A stage that is not unlit.” The full model produces stable, correctly lit stage scenes. Removing repulsive energy weakens negation enforcement and introduces temporal instability (e.g., lighting flicker), while removing constraint scheduling disrupts early-stage structure formation, causing scale drift and unnatural light-source placement.

ance arises from the constraint formulation rather than incidental prompt alignment. Removing constraint scheduling degrades both global alignment and negation stability, reducing CLIPScore and increasing CLIP-neg. This indicates that temporally modulated constraint strength is essential to prevent interference with early structural formation while ensuring late-stage suppression. Importantly, the same trend is observed under direct vision-language evaluation. Both ablations reduce the Negation Compliance Score (NCS) and increase the Negation Violation Rate (NVR), confirming that the observed degradation is not limited to embedding-space metrics but reflects genuine semantic vi-

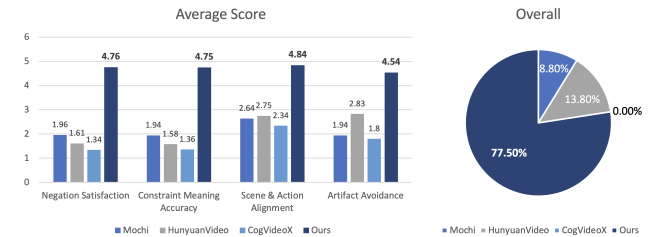


Figure 5. **User study results for negation-aware video generation.** 50 participants evaluated four anonymized methods across four criteria: *Negation Satisfaction*, *Constraint Meaning Accuracy*, *Scene & Action Alignment*, and *Artifact Avoidance* (left). Our method consistently achieved the highest average ratings across all dimensions (4.54–4.84), substantially outperforming Mochi, HunyuanVideo, and CogVideoX. In the overall preference comparison (right), **77.5%** of votes favored our method, compared to 13.8% for HunyuanVideo, 8.8% for Mochi, and 0.0% for CogVideoX.

olations under multimodal reasoning. Figure 4 further illustrates distinct failure modes of the two ablations. **More detailed quantitative and qualitative analysis are provided in Appendix E.**

4.6. User Study

We conducted a user study with 50 participants to assess perceptual quality and negation compliance in video generation. For each of eight prompts, participants were shown four anonymized results generated by Mochi, HunyuanVideo, CogVideoX, and *Ours*, with presentation order randomized per question to prevent positional bias. Participants rated each output on four 5-point Likert criteria: (1) *Negation Satisfaction*, (2) *Constraint Meaning Accuracy*, (3) *Scene & Action Alignment*, and (4) *Artifact Avoidance*, and additionally selected an overall preferred result. As illustrated in Figure 5, our method achieved the highest mean scores across all axes, reaching 4.76 (negation satisfaction),

4.75 (constraint meaning accuracy), 4.84 (scene alignment), and 4.54 (artifact avoidance), while competing methods remained near the disagreement range (1.34–2.83). In overall preference, **77.5%** of votes favored *Ours*, indicating a clear perceptual advantage over existing methods. These findings suggest that modeling linguistic negation as a constrained diffusion process substantially improves semantic compliance and visual fidelity. **See Appendix F for full user study details.**

5. Conclusions, Limitations and Future Work

This work presents the first generative formulation of *linguistic negation* in vision-language models (VLMs). While prior studies have shown that VLMs struggle to distinguish affirmative and negated captions at the representation level, negation has not previously been formalized as part of the generative process itself. We shift the perspective from embedding separability to trajectory-level semantic control, modeling negation as a structured feasibility condition over neural generation dynamics. Our formulation provides a unified treatment of diverse negation phenomena—including structural functional negation (SFN), graded non-inversion semantics, double negation sensitivity (DNS), and scoped negation disambiguation (SND)—within a single constraint-based framework. Rather than introducing new architectures or retraining large models, we demonstrate how linguistic structure can be translated into geometric constraints on semantic update directions, enabling logically consistent generation. Importantly, this perspective extends beyond static image synthesis. Because constraints are enforced at the level of neural trajectory evolution, the formulation naturally applies to temporally evolving video generation and, more broadly, suggests extensions toward vision-language-action (VLA) systems where language constrains both perception and behavior. By treating linguistic negation as a principled semantic operator rather than a prompt heuristic, we establish a new research direction at the intersection of formal semantics and neural generative modeling. This work positions linguistic constraint modeling—not diffusion heuristics—as the central challenge for next-generation vision-language systems.

Limitations & Future Work. Our current formulation approximates linguistic constraints within a tractable geometric structure over semantic update directions. Certain forms of pragmatically inferred or world-knowledge-dependent negation may require richer semantic parsing and non-linear constraint modeling. Additionally, constraint effectiveness depends on the fidelity of the underlying vision-language representation space. Future work may extend this formulation beyond negation to broader classes of linguistic operators, including quantification, modality, and compositional logical structure. Integrating formal semantic

representations with neural trajectory control could further bridge symbolic linguistic theory and large-scale generative models. More broadly, viewing neural generation as a constrained dynamical process opens new directions for logically grounded reasoning in image, video, and vision-language-action systems.

References

- [1] Genmo AI. Mochi-1 preview. <https://huggingface.co/genmo/mochi-1-preview>, 2024. 6
- [2] Kumail Alhamoud, Shaden Alshammari, Yonglong Tian, Guohao Li, Philip HS Torr, Yoon Kim, and Marzyeh Ghassemi. Vision-language models do not understand negation. In *Proceedings of the Computer Vision and Pattern Recognition Conference*, pages 29612–29622, 2025. 1, 3
- [3] Omer Bar-Tal, Hila Chefer, Omer Tov, Charles Herrmann, Roni Paiss, Shiran Zada, Ariel Ephrat, Junhwa Hur, Guanghui Liu, Amit Raj, et al. Lumiere: A space-time diffusion model for video generation. In *SIGGRAPH Asia 2024 Conference Papers*, pages 1–11, 2024. 3
- [4] Logan E Beaver. Lq-ocp: Energy-optimal control for lq problems. In *2024 American Control Conference (ACC)*, pages 821–826. IEEE, 2024. 3
- [5] Andreas Blattmann, Tim Dockhorn, Sumith Kulal, Daniel Mendeleevitch, Maciej Kilian, Dominik Lorenz, Yam Levi, Zion English, Vikram Voleti, Adam Letts, et al. Stable video diffusion: Scaling latent video diffusion models to large datasets. *arXiv preprint arXiv:2311.15127*, 2023. 3
- [6] Andreas Blattmann, Robin Rombach, Huan Ling, Tim Dockhorn, Seung Wook Kim, Sanja Fidler, and Karsten Kreis. Align your latents: High-resolution video synthesis with latent diffusion models. In *Proceedings of the IEEE/CVF conference on computer vision and pattern recognition*, pages 22563–22575, 2023. 3
- [7] Hila Chefer, Yuval Alaluf, Yael Vinker, Lior Wolf, and Daniel Cohen-Or. Attend-and-excite: Attention-based semantic guidance for text-to-image diffusion models. *ACM transactions on Graphics (TOG)*, 42(4):1–10, 2023. 1
- [8] Weifeng Chen, Yatai Ji, Jie Wu, Hefeng Wu, Pan Xie, Jiashi Li, Xin Xia, Xuefeng Xiao, and Liang Lin. Control-a-video: Controllable text-to-video generation with diffusion models. *arXiv e-prints*, pages arXiv–2305, 2023. 3
- [9] Xinyuan Chen, Yaohui Wang, Lingjun Zhang, Shaobin Zhuang, Xin Ma, Jiashuo Yu, Yali Wang, Dahua Lin, Yu Qiao, and Ziwei Liu. Seine: Short-to-long video diffusion model for generative transition and prediction. In *The Twelfth International Conference on Learning Representations*, 2023.
- [10] Hao Fei, Shengqiong Wu, Wei Ji, Hanwang Zhang, and Tat-Seng Chua. Dysen-vdm: Empowering dynamics-aware text-to-video diffusion with llms. In *Proceedings of the IEEE/CVF Conference on Computer Vision and Pattern Recognition*, pages 7641–7653, 2024. 3
- [11] Weixi Feng, Xuehai He, Tsu-Jui Fu, Varun Jampani, Arjun Akula, Pradyumna Narayana, Sugato Basu, Xin Eric Wang, and William Yang Wang. Training-free structured diffusion

- guidance for compositional text-to-image synthesis. *arXiv preprint arXiv:2212.05032*, 2022. 3
- [12] Kuzman Ganchev, Joao Graça, Jennifer Gillenwater, and Ben Taskar. Posterior regularization for structured latent variable models. *The Journal of Machine Learning Research*, 11: 2001–2049, 2010. 3
- [13] Rohit Gandikota, Joanna Materzynska, Jaden Fiotto-Kaufman, and David Bau. Erasing concepts from diffusion models. In *Proceedings of the IEEE/CVF international conference on computer vision*, pages 2426–2436, 2023. 3
- [14] Rohit Gandikota, Hadas Orgad, Yonatan Belinkov, Joanna Materzyńska, and David Bau. Unified concept editing in diffusion models. In *Proceedings of the IEEE/CVF winter conference on applications of computer vision*, pages 5111–5120, 2024. 3
- [15] Songwei Ge, Seungjun Nah, Guilin Liu, Tyler Poon, Andrew Tao, Bryan Catanzaro, David Jacobs, Jia-Bin Huang, Ming-Yu Liu, and Yogesh Balaji. Preserve your own correlation: A noise prior for video diffusion models. In *Proceedings of the IEEE/CVF International Conference on Computer Vision*, pages 22930–22941, 2023. 3
- [16] Rohit Girdhar, Mannat Singh, Andrew Brown, Quentin Duval, Samaneh Azadi, Sai Saketh Rambhatla, Akbar Shah, Xi Yin, Devi Parikh, and Ishan Misra. Emu video: Factorizing text-to-video generation by explicit image conditioning. *arXiv preprint arXiv:2311.10709*, 2023.
- [17] Yingqing He, Tianyu Yang, Yong Zhang, Ying Shan, and Qifeng Chen. Latent video diffusion models for high-fidelity long video generation. *arXiv preprint arXiv:2211.13221*, 2022.
- [18] Roberto Henschel, Levon Khachatryan, Daniil Hayrapetyan, Hayk Poghosyan, Vahram Tadevosyan, Zhangyang Wang, Shant Navasardyan, and Humphrey Shi. Streaming2v: Consistent, dynamic, and extendable long video generation from text. *arXiv preprint arXiv:2403.14773*, 2024. 3
- [19] Jonathan Ho, William Chan, Chitwan Saharia, Jay Whang, Ruiqi Gao, Alexey Gritsenko, Diederik P Kingma, Ben Poole, Mohammad Norouzi, David J Fleet, et al. Imagen video: High definition video generation with diffusion models. *arXiv preprint arXiv:2210.02303*, 2022. 3
- [20] Cheng-Yu Hsieh, Jieyu Zhang, Zixian Ma, Aniruddha Kembhavi, and Ranjay Krishna. Sugarcrepe: Fixing hackable benchmarks for vision-language compositionality. *Advances in neural information processing systems*, 36:31096–31116, 2023. 3
- [21] Barbara Kaup, Jana Lüttke, and Rolf A Zwaan. Processing negated sentences with contradictory predicates: Is a door that is not open mentally closed? *Journal of Pragmatics*, 38(7):1033–1050, 2006. 1, 3
- [22] Barbara Kaup, Richard H Yaxley, Carol J Madden, Rolf A Zwaan, and Jana Lüttke. Experiential simulations of negated text information. *Quarterly journal of experimental psychology*, 60(7):976–990, 2007. 1, 3
- [23] Levon Khachatryan, Andranik Movsisyan, Vahram Tadevosyan, Roberto Henschel, Zhangyang Wang, Shant Navasardyan, and Humphrey Shi. Text2video-zero: Text-to-image diffusion models are zero-shot video generators. In *Proceedings of the IEEE/CVF International Conference on Computer Vision*, pages 15954–15964, 2023. 3
- [24] Weijie Kong, Qi Tian, Zijian Zhang, Rox Min, Zuozhuo Dai, Jin Zhou, Jiangfeng Xiong, Xin Li, Bo Wu, Jianwei Zhang, et al. Hunyuanvideo: A systematic framework for large video generative models. *arXiv preprint arXiv:2412.03603*, 2024. 3
- [25] Long Lian, Baifeng Shi, Adam Yala, Trevor Darrell, and Boyi Li. Llm-grounded video diffusion models. *arXiv preprint arXiv:2309.17444*, 2023. 3
- [26] Nan Liu, Shuang Li, Yilun Du, Antonio Torralba, and Joshua B Tenenbaum. Compositional visual generation with composable diffusion models. In *European conference on computer vision*, pages 423–439. Springer, 2022. 3
- [27] Gyeongrok Oh, Jaehwan Jeong, Sieun Kim, Wonmin Byeon, Jinkyu Kim, Sungwoong Kim, and Sangpil Kim. Mevg: Multi-event video generation with text-to-video models. In *European Conference on Computer Vision*, pages 401–418. Springer, 2024. 3
- [28] OpenAI. Video generation models as world simulators. <https://openai.com/index/video-generation-models-as-world-simulators/>, 2024.
- [29] Adam Polyak, Amit Zohar, Andrew Brown, Andros Tjandra, Animesh Sinha, Ann Lee, Apoorv Vyas, Bowen Shi, Chih-Yao Ma, Ching-Yao Chuang, David Yan, Dhruv Choudhary, DingKang Wang, Geet Sethi, Guan Pang, Haoyu Ma, Ishan Misra, Ji Hou, Jialiang Wang, Kiran Jagadeesh, Kungpeng Li, Luxin Zhang, Mannat Singh, Mary Williamson, Matt Le, Matthew Yu, Mitesh Kumar Singh, Peizhao Zhang, Peter Vajda, Quentin Duval, Rohit Girdhar, Roshan Sumbaly, Sai Saketh Rambhatla, Sam Tsai, Samaneh Azadi, Samyak Datta, Sanyuan Chen, Sean Bell, Sharadh Ramaswamy, Shelly Sheynin, Siddharth Bhattacharya, Simran Motwani, Tao Xu, Tianhe Li, Tingbo Hou, Wei-Ning Hsu, Xi Yin, Xi-aoliang Dai, Yaniv Taigman, Yaqiao Luo, Yen-Cheng Liu, Yi-Chiao Wu, Yue Zhao, Yuval Kirstain, Zecheng He, Zijian He, Albert Pumarola, Ali Thabet, Arsiom Sanakoyeu, Arun Mallya, Baishan Guo, Boris Araya, Breena Kerr, Carleigh Wood, Ce Liu, Cen Peng, Dimitry Vengertsev, Edgar Schonfeld, Elliot Blanchard, Felix Juefei-Xu, Fraylie Nord, Jeff Liang, John Hoffman, Jonas Kohler, Kaolin Fire, Karthik Sivakumar, Lawrence Chen, Licheng Yu, Luya Gao, Markos Georgopoulos, Rashel Moritz, Sara K. Sampson, Shikai Li, Simone Parmeggiani, Steve Fine, Tara Fowler, Vladan Petrovic, and Yuming Du. Movie gen: A cast of media foundation models, 2025.
- [30] Zhiwu Qing, Shiwei Zhang, Jiayu Wang, Xiang Wang, Yujie Wei, Yingya Zhang, Changxin Gao, and Nong Sang. Hierarchical spatio-temporal decoupling for text-to-video generation. In *Proceedings of the IEEE/CVF Conference on Computer Vision and Pattern Recognition*, pages 6635–6645, 2024.
- [31] Haonan Qiu, Menghan Xia, Yong Zhang, Yingqing He, Xintao Wang, Ying Shan, and Ziwei Liu. Freenoise: Tuning-free longer video diffusion via noise rescheduling. *arXiv preprint arXiv:2310.15169*, 2023. 3

- [32] Royi Rassin, Eran Hirsch, Daniel Glickman, Shauli Ravfogel, Yoav Goldberg, and Gal Chechik. Linguistic binding in diffusion models: Enhancing attribute correspondence through attention map alignment. *Advances in Neural Information Processing Systems*, 36:3536–3559, 2023. 3
- [33] Abhishek Sharma, Adams Yu, Ali Razavi, Andeep Toor, Andrew Pierson, Ankush Gupta, Austin Waters, Aäron van den Oord, Daniel Tanis, Dumitru Erhan, Eric Lau, Eleni Shaw, Gabe Barth-Maron, Greg Shaw, Han Zhang, Henna Nandwani, Hernan Moraldo, Hyunjik Kim, Irina Blok, Jakob Bauer, Jeff Donahue, Junyoung Chung, Kory Mathewson, Kurtis David, Lasse Espeholt, Marc van Zee, Matt McGill, Medhini Narasimhan, Miaosen Wang, Mikołaj Bińkowski, Mohammad Babaeizadeh, Mohammad Taghi Saffar, Nando de Freitas, Nick Pezzotti, Pieter-Jan Kindermans, Poorva Rane, Rachel Hornung, Robert Riachi, Ruben Villegas, Rui Qian, Sander Dieleman, Serena Zhang, Serkan Cabi, Shixin Luo, Shlomi Fruchter, Signe Nørly, Srivatsan Srinivasan, Tobias Pfaff, Tom Hume, Vikas Verma, Weizhe Hua, William Zhu, Xinchen Yan, Xinyu Wang, Yelin Kim, Yuqing Du, and Yutian Chen. Veo. 2024. 3
- [34] Uriel Singer, Adam Polyak, Thomas Hayes, Xi Yin, Jie An, Songyang Zhang, Qiyuan Hu, Harry Yang, Oron Ashual, Oran Gafni, et al. Make-a-video: Text-to-video generation without text-video data. *arXiv preprint arXiv:2209.14792*, 2022. 3
- [35] Jaisidh Singh, Ishaan Shrivastava, Mayank Vatsa, Richa Singh, and Aparna Bharati. Learn” no” to say” yes” better: Improving vision-language models via negations. *arXiv preprint arXiv:2403.20312*, 2024. 1, 3
- [36] Tristan Thrush, Ryan Jiang, Max Bartolo, Amanpreet Singh, Adina Williams, Douwe Kiela, and Candace Ross. Winoground: Probing vision and language models for visiolinguistic compositionality. In *Proceedings of the IEEE/CVF Conference on Computer Vision and Pattern Recognition*, pages 5238–5248, 2022. 3
- [37] Veo-Team, :, Agrim Gupta, Ali Razavi, Andeep Toor, Ankush Gupta, Dumitru Erhan, Eleni Shaw, Eric Lau, Frank Belletti, Gabe Barth-Maron, Gregory Shaw, Hakan Erdogan, Hakim Sidahmed, Henna Nandwani, Hernan Moraldo, Hyunjik Kim, Irina Blok, Jeff Donahue, José Lezama, Kory Mathewson, Kurtis David, Matthieu Kim Lorrain, Marc van Zee, Medhini Narasimhan, Miaosen Wang, Mohammad Babaeizadeh, Nelly Papalampidi, Nick Pezzotti, Nilpa Jha, Parker Barnes, Pieter-Jan Kindermans, Rachel Hornung, Ruben Villegas, Ryan Poplin, Salah Zaiem, Sander Dieleman, Sayna Ebrahimi, Scott Wisdom, Serena Zhang, Shlomi Fruchter, Signe Nørly, Weizhe Hua, Xinchen Yan, Yuqing Du, and Yutian Chen. Veo 2. 2024. 3
- [38] Ruben Villegas, Mohammad Babaeizadeh, Pieter-Jan Kindermans, Hernan Moraldo, Han Zhang, Mohammad Taghi Saffar, Santiago Castro, Julius Kunze, and Dumitru Erhan. Phenaki: Variable length video generation from open domain textual description. *arXiv preprint arXiv:2210.02399*, 2022.
- [39] Fu-Yun Wang, Wenshuo Chen, Guanglu Song, Han-Jia Ye, Yu Liu, and Hongsheng Li. Gen-l-video: Multi-text to long video generation via temporal co-denoising. *arXiv preprint arXiv:2305.18264*, 2023.
- [40] Jiuniu Wang, Hangjie Yuan, Dayou Chen, Yingya Zhang, Xiang Wang, and Shiwei Zhang. Modelscope text-to-video technical report. *arXiv preprint arXiv:2308.06571*, 2023.
- [41] Yaohui Wang, Xinyuan Chen, Xin Ma, Shangchen Zhou, Ziqi Huang, Yi Wang, Ceyuan Yang, Yinan He, Jiashuo Yu, Peiqing Yang, et al. Lavie: High-quality video generation with cascaded latent diffusion models. *International Journal of Computer Vision*, pages 1–20, 2024.
- [42] Wenming Weng, Ruoyu Feng, Yanhui Wang, Qi Dai, Chunyu Wang, Dacheng Yin, Zhiyuan Zhao, Kai Qiu, Jianmin Bao, Yuhui Yuan, et al. Art-v: Auto-regressive text-to-video generation with diffusion models. In *Proceedings of the IEEE/CVF Conference on Computer Vision and Pattern Recognition*, pages 7395–7405, 2024.
- [43] Bing Wu, Chang Zou, Changlin Li, DuoJun Huang, Fang Yang, Hao Tan, Jack Peng, Jianbing Wu, Jiangfeng Xiong, Jie Jiang, et al. Hunyuanvideo 1.5 technical report. *arXiv preprint arXiv:2511.18870*, 2025. 3
- [44] Junhao Xiao, Zhiyu Wu, Hao Lin, Yi Chen, Yahui Liu, Xiaoran Zhao, Zixu Wang, and Zejiang He. Not just what’s there: Enabling clip to comprehend negated visual descriptions without fine-tuning. *arXiv preprint arXiv:2602.21035*, 2026. 1, 3
- [45] Xin Xie and Dong Gong. Dymo: Training-free diffusion model alignment with dynamic multi-objective scheduling. In *Proceedings of the Computer Vision and Pattern Recognition Conference*, pages 13220–13230, 2025. 1
- [46] Shengming Yin, Chenfei Wu, Huan Yang, Jianfeng Wang, Xiaodong Wang, Minheng Ni, Zhengyuan Yang, Linjie Li, Shuguang Liu, Fan Yang, et al. Nuwa-xl: Diffusion over diffusion for extremely long video generation. *arXiv preprint arXiv:2303.12346*, 2023. 3
- [47] Mert Yuksekogun, Federico Bianchi, Pratyusha Kalluri, Dan Jurafsky, and James Zou. When and why vision-language models behave like bags-of-words, and what to do about it? *arXiv preprint arXiv:2210.01936*, 2022. 3
- [48] Stefano Zampini, Jacob K Christopher, Luca Oneto, Davide Anguita, and Ferdinando Fioretto. Training-free constrained generation with stable diffusion models. *arXiv preprint arXiv:2502.05625*, 2025. 1, 3
- [49] David Junhao Zhang, Jay Zhangjie Wu, Jia-Wei Liu, Rui Zhao, Lingmin Ran, Yuchao Gu, Difei Gao, and Mike Zheng Shou. Show-1: Marrying pixel and latent diffusion models for text-to-video generation. *International Journal of Computer Vision*, pages 1–15, 2024. 3
- [50] Jichen Zhang, Liqun Zhao, Antonis Papachristodoulou, and Jack Umenberger. Constrained diffusers for safe planning and control. *arXiv preprint arXiv:2506.12544*, 2025. 1, 3
- [51] Yabo Zhang, Yuxiang Wei, Dongsheng Jiang, Xiaopeng Zhang, Wangmeng Zuo, and Qi Tian. Controlvideo: Training-free controllable text-to-video generation. *arXiv preprint arXiv:2305.13077*, 2023. 3
- [52] Yuhui Zhang, Yuchang Su, Yiming Liu, and Serena Yeung-Levy. Negvqa: Can vision language models understand negation? In *Findings of the Association for Computational Linguistics: ACL 2025*, pages 3707–3716, 2025. 3

A. Ethics Statement

Ethics Statement

This work proposes a training-free, constraint-based formulation of linguistic negation for vision-language generation by projecting diffusion guidance updates onto a feasible set derived from prompt structure, with the goal of improving logical faithfulness and safety-relevant exclusion behavior in text-to-image and text-to-video systems; as with all generative models, the approach may be misused to create deceptive or harmful media, and improved controllability should not be conflated with policy compliance, since harmful content can still be produced if prompted, so the method is not a universal safety solution but a mechanism for enforcing structured constraints when user intent and downstream policy are aligned; because our framework operates entirely on frozen pretrained backbones, it inherits representational biases and uneven concept coverage from underlying models and datasets, and constraint effectiveness may vary across concepts or contexts, so improvements in negation compliance do not imply fairness guarantees; we introduce a structured negation-centric benchmark used exclusively for evaluation (not training), designed to probe linguistic structure rather than elicit sensitive or targeted content, and we recommend that future extensions avoid prompts involving protected groups, disallowed activities, or identity-based inference; the reported user study involved adult participants (18+) recruited through open online channels, participation was voluntary and anonymous, no personally identifying information was collected, results are reported only in aggregate, and the study protocol was reviewed by University of Maryland’s Institutional Review Board (IRB) (Kuali-IRB Number #1179-1) and determined to qualify for exemption (45 CFR Part 46 – Protection of Human Subjects) under applicable regulations; from an environmental and transparency perspective, we report computation time and peak memory consumption for all configurations, and because our approach introduces no additional training and operates at inference time without architectural modification, it does not incur retraining overhead beyond standard diffusion inference; overall, we believe that trajectory-level modeling of linguistic operators can improve reliability and constraint consistency in generative systems, while emphasizing that responsible deployment requires appropriate content policies, safeguards, and auditing procedures.

B. Detailed Benchmarking Datasets

Unlike prior works that evaluate negation understanding in vision-language representations, our objective is to assess *negation compliance in generative diffusion trajectories*. This distinction fundamentally changes the role of datasets in our evaluation protocol.

Why Standard Datasets Are Insufficient. Conventional vision-language benchmarks such as MS-COCO, CC, or Web-Vid are designed for descriptive captioning and semantic alignment. Negation-specific prompts are **rare, incidental, and not systematically structured**. More importantly, these datasets are intended to evaluate **representation separability or retrieval consistency**, rather than distributional behavior of generated samples under negation constraints.

In representation learning settings, the evaluation question typically takes the form:

$$S(I, T_{\text{pos}}) > S(I, T_{\text{neg}})$$

which measures embedding separability. In contrast, our problem is generative and distributional:

$$\mathbb{P}_{x_0 \sim p_{\theta}(\cdot|y)} [\text{negated concept appears}].$$

Standard datasets such as NegCLIP, CC-Neg, and ARO **do not provide structured prompts to measure this probability, nor do they capture temporal emergence of forbidden content in video diffusion**. Therefore, using them directly would neither test nor reveal the core property studied in this work: constraint enforcement during generation.

For this reason, we construct a controlled negation-centric evaluation suite designed explicitly to probe generative behavior under negation constraints. Importantly, this dataset is used solely for evaluation; no training or fine-tuning is performed.

Dataset Scale. For each of the eight categories described below, we construct 50 prompt pairs, resulting in a total of 400 evaluation sets. Each set consists of structured prompts designed to probe negation compliance under controlled conditions. Rather than maximizing prompt volume, our benchmark prioritizes linguistic precision and categorical coverage. Each of

the 50 prompts per category is carefully designed to isolate the target negation phenomenon, preventing confounding factors from adjacent linguistic categories. All quantitative results reported in the main paper are computed over this benchmark. The dataset is used exclusively for evaluation; no training or fine-tuning is performed.

Design Principles. Our benchmarking suite is built around eight complementary categories, each targeting a distinct dynamical or linguistic failure mode observed in text-to-video diffusion models. The categories are constructed to (1) isolate negation as a primary semantic constraint, (2) prevent trivial prompt-engineering solutions, (3) expose trajectory-level violations that may emerge temporally, and (4) disentangle linguistic phenomena such as graded negation, compositional structure, and scope ambiguity from purely object-level suppression.

(1) AOC: Absent Object Consistency

The Absent Object Consistency (AOC) set evaluates whether explicitly negated objects remain absent throughout the entire video. Prompts follow the structure:

“A [scene] with no [object].”

Representative example:

“A highway at sunset, with **no** vehicles.”
“A city skyline at night, with **no** lights on.”
“A snowfield, with **no** footprints.”

In video diffusion models, forbidden objects frequently emerge in later frames even if absent initially. This set directly measures temporal consistency of negation compliance. It isolates the simplest but most critical form of negation: object absence.

(2) LEN: Late Emergence Negation

The Late Emergence Negation (LEN) set targets a common trajectory-level failure mode: negated content appearing only after structural formation. Prompts introduce gradual scene evolution:

“A concert stage lighting up, with **no** performers.”
“A ski slope after snowfall, with **no** ski tracks appearing.”
“A dock at dusk, with **no** ropes appearing.”

Such prompts test whether time-dependent constraint scheduling successfully prevents semantic drift during later diffusion stages. This category is particularly important for video models, where temporal hallucination is prevalent.

(3) INA: Implicit Natural-only Attribute

The Implicit Natural-only Attribute (INA) set evaluates negation under *semantic exclusivity* rather than explicit lexical negation. Instead of prompts of the form “with no [object],” INA specifies a closed category whose elements are exhaustive. Representative example:

“A scene featuring **only** natural elements.”
“A meadow under the night sky with **only** grass and stars.”
“A natural cave interior featuring **only** stone and shadows.”

In this formulation, exclusion must be inferred from the semantic scope of “only.” The prompt implicitly prohibits humans, vehicles, buildings, and other artificial structures without enumerating them. This design tests whether the model suppresses objects that are statistically likely under scene priors but logically disallowed by category closure.

Formally, let $\mathcal{C}_{\text{allowed}}$ denote the semantically closed set implied by the prompt and $\mathcal{C}_{\text{prior}}$ denote high-probability co-occurring objects under the generative prior. In many natural scenes,

$$\mathcal{C}_{\text{prior}} \not\subset \mathcal{C}_{\text{allowed}},$$

creating a conflict between prior likelihood and semantic constraint. INA evaluates whether the model suppresses objects in

$$\mathcal{C}_{\text{prior}} \setminus \mathcal{C}_{\text{allowed}},$$

without relying on explicit negation markers.

Unlike AOC, which measures explicit object absence, INA probes the model’s ability to enforce logically implied exclusions under strong co-occurrence bias.

(4) MNC: Multi-Negation Composition

The Multi-Negation Composition (MNC) set evaluates compositional robustness under multiple simultaneous constraints:

- “A classroom scene with **no** students, **no** teacher, and **no** books.”
- “A mountain cabin with **no** doors, **no** windows, and **no** chimney.”
- “A snow-covered road with **no** tire tracks, **no** signs, and **no** vehicles.”

This setting probes whether repulsive energies combine stably without degrading generation quality or causing constraint collapse. Representation-based negation learning often struggles under multiple exclusions due to similarity conflicts; MNC tests the stability of trajectory-level control under compounded constraints.

(5) SFN: Structural Functional Negation

Structural Functional Negation (SFN) evaluates negation over actions or states rather than object existence:

- “A person holding a phone but **not** using it.”
- “A clock ticking but **not** moving its hands.”
- “A factory assembly line active but **not** producing items.”

Here, the object must remain present while a specific action is suppressed. This category differentiates between simple object removal and higher-order semantic control. It tests whether negation-aware diffusion can modulate behavior-level attributes without eliminating the underlying entity.

(6) NMI: Non-Inversion Mitigation

The Non-Inversion Mitigation (NMI) set evaluates cases where negation does not correspond to strict semantic inversion. In natural language, expressions such as “not bad” or “not uncommon” do not necessarily imply the opposite extreme (e.g., “excellent” or “rare”), but instead express moderated or context-dependent meanings.

- “A dog that is **not** aggressive.”
- “A harbor that is **not** fully occupied.”
- “A mountain peak that is **not** completely snow-covered.”

These prompts require the model to attenuate specific attributes rather than completely eliminate or invert them. A naive repulsive formulation may over-correct, producing semantically exaggerated opposites (e.g., empty beach, extremely casual meal).

Formally, this category probes whether negation enforcement behaves as a *bounded constraint* rather than a binary complement operation. Let A denote a continuous attribute (e.g., crowdedness). Instead of enforcing $A = 0$, NMI requires:

$$A(x_t) \leq \tau,$$

where τ represents a moderation threshold rather than strict absence. This category evaluates whether the generative trajectory respects graded semantic constraints without collapsing to degenerate extremes.

(7) DNS: Double Negation Sensitivity

The Double Negation Sensitivity (DNS) set evaluates prompts containing multiple nested or compositional negations. In natural language, double negation may either cancel (logical double negation) or intensify negation depending on linguistic context.

- “A stage that is **not** *unlit*.”
- “A beach that is **not** *shell-less*.”
- “A rooftop that is **not** *vent-less*.”

Primary negation cues are highlighted in **bold**, while secondary negation operators (e.g., *unlit*, *-less*) are shown in *italics* to illustrate compositional negation structure.

In these cases, naive repulsive composition may lead to attraction–repulsion conflicts, over-suppression, or unstable semantic oscillation. DNS tests whether the control mechanism correctly resolves nested negation structure without generating contradictory or degenerate outputs.

From a constraint perspective, this set examines whether sequential negations yield consistent feasible regions rather than competing gradient directions. It specifically probes robustness of the minimal-energy correction mechanism under sign-sensitive semantic composition.

Method	CLIPScore \uparrow	CLIP-neg \downarrow	BLIP \uparrow	DINO-conf \downarrow	NCS \uparrow	NVR \downarrow
Mochi	0.2857 \pm 0.0196	0.2411 \pm 0.0288	0.8183 \pm 0.0774	0.0175 \pm 0.0314	3.5789 \pm 1.8548	0.3625 \pm 0.4813
HunyuanVideo	0.2743 \pm 0.0360	0.2620 \pm 0.0388	0.7776 \pm 0.1018	0.0184 \pm 0.0268	3.4584 \pm 1.8712	0.3675 \pm 0.4827
CogVideoX	0.2836 \pm 0.0320	0.2442 \pm 0.0414	0.7869 \pm 0.0984	0.0181 \pm 0.0269	3.4080 \pm 1.8828	0.3800 \pm 0.4859
Ours (Full Model)	0.2924 \pm 0.0225	0.2336 \pm 0.0231	0.8201 \pm 0.0729	0.0167 \pm 0.0278	4.0700 \pm 1.6406	0.2300 \pm 0.4213
Ours w/o Repulsive Energy	0.2924 \pm 0.0221	0.2411 \pm 0.0281	0.8128 \pm 0.0756	0.0181 \pm 0.0301	3.9548 \pm 1.6724	0.2625 \pm 0.4405
Ours w/o Constraint Scheduling	0.2800 \pm 0.0305	0.2405 \pm 0.0477	0.7869 \pm 0.0881	0.0174 \pm 0.0245	3.5789 \pm 1.8439	0.3625 \pm 0.4813

Table 2. **Detailed quantitative evaluation with mean and standard deviation.** All metrics are reported as mean \pm standard deviation over the full evaluation set. NCS denotes the Negation Compliance Score obtained from a direct vision-language judge, and NVR denotes the Negation Violation Rate computed from the judge’s binary forbidden-presence decision.

(8) SND: Scoped Negation Disambiguation

The Scoped Negation Disambiguation (SND) set evaluates the model’s ability to correctly identify the semantic scope of negation within structurally ambiguous sentences. Unlike SFN, which suppresses a specific action while preserving object presence, SND focuses on determining *which component* of the sentence is negated.

“A teacher *helping* a student who is **not** paying attention.”

“A boat anchored near an island that is **not** *inhabited*.”

“A robot next to a screen that is **not** *displaying content*.”

Negation cues are highlighted in **bold**, while the negated semantic targets are shown in *italics*.

In these prompts, negation applies to a specific subordinate clause or attribute. Incorrect scope resolution may lead to suppression of the wrong entity (e.g., removing the dog instead of stopping its motion).

Formally, let $g_i(x_t)$ denote candidate semantic components. Scope detection determines which g_i participates in the constraint:

$$g_{i^*}(x_t) \leq \varepsilon,$$

while leaving other components unconstrained. This dataset isolates linguistic disambiguation from functional negation (SFN) by requiring correct identification of the constrained semantic variable rather than merely suppressing an action.

Summary. Together, AOC, LEN, INA, MNC, SFN, NMI, DNS, and SND form a structured evaluation suite that probes multiple dimensions of negation-aware generation, including object absence, temporal stability, implicit semantic exclusion, compositional robustness, functional suppression, graded non-inversion semantics, nested negation consistency, and scope-sensitive constraint identification. These categories are deliberately designed to reflect distinct dynamical and linguistic failure modes in generative diffusion models. By isolating these complementary dimensions, the benchmark provides a targeted and interpretable evaluation of constraint-consistent diffusion trajectory control under both explicit and structurally complex negation.

C. Detailed Qualitative Results

Figures 6, 7, and 8 (Detailed close-up results are shown in Figures 9–32) presents qualitative comparisons across eight negation categories, spanning simple object absence (AOC, MNC), logical exclusion (LEN), implicit constraints (INA), functional negation (SFN), moderated semantic negation (NMI), double negation (DNS), and scoped relational negation (SND).

In straightforward absence settings such as AOC (“no vehicles”) and MNC (“no students, no teacher, no books”), baseline models often partially retain forbidden objects or introduce subtle artifacts, whereas our model cleanly suppresses negated entities without degrading global scene realism.

In functional and behavioral negation (SFN), where the object must remain present but unused, baseline methods frequently collapse the constraint into object removal or unintended action depiction. In contrast, our model preserves the object while suppressing the prohibited interaction, demonstrating behavior-level control beyond simple deletion.

More complex logical structures further highlight the differences. In DNS (“not unlit”), baseline models misinterpret the double negation and generate dark stages, reflecting semantic inversion. Our model correctly resolves the logical structure, producing a stably illuminated stage. In SND (“student who is not paying attention”), competing models often misplace the

negation scope, incorrectly applying inattentiveness to the teacher or failing to represent the relational constraint. Our model maintains proper entity roles while enforcing the scoped negation.

Across all categories, competing diffusion models exhibit either semantic leakage (failure to suppress forbidden concepts), structural distortion, or scope misinterpretation. In contrast, our model consistently enforces negation as a structured constraint on diffusion dynamics, preserving global scene composition while satisfying complex linguistic conditions.

D. Detailed Quantitative Evaluation

We evaluate whether generated videos satisfy the full textual constraint using standard, widely adopted metrics without modifying prompts or introducing threshold-based decision rules. Our evaluation focuses exclusively on prompt satisfaction: whether the generated video aligns with the intended semantics while respecting negation constraints.

CLIPScore. We compute CLIPScore by measuring cosine similarity between each generated frame and the full textual prompt, including negation phrases. For a video consisting of T frames $\{I_t\}_{t=1}^T$ and prompt P , we compute

$$\text{CLIPScore} = \frac{1}{T} \sum_{t=1}^T \cos(E_{\text{img}}(I_t), E_{\text{text}}(P)).$$

Higher CLIPScore indicates stronger global alignment between the generated video and the intended textual description.

CLIP Similarity to Negated Concept (CLIP-neg). To measure negation compliance, we compute the cosine similarity between generated frames and the explicitly negated concept c_{neg} :

$$\text{CLIP-neg} = \frac{1}{T} \sum_{t=1}^T \cos(E_{\text{img}}(I_t), E_{\text{text}}(c_{\text{neg}})).$$

Lower CLIP-neg values indicate stronger suppression of the forbidden concept. Importantly, this metric uses the standard CLIP similarity formulation without thresholding or manual intervention.

BLIP Caption Alignment. We further evaluate semantic fidelity using BLIP-based captioning. For each frame, we generate a caption \hat{C}_t using a pretrained BLIP model and compute its similarity to the original prompt:

$$\text{BLIP} = \frac{1}{T} \sum_{t=1}^T \cos(E_{\text{text}}(\hat{C}_t), E_{\text{text}}(P)).$$

This provides a complementary text-level consistency measure based on generated descriptions rather than direct image-text matching.

DINO Detection Confidence. To directly assess object presence, we use an open-vocabulary detection model (e.g., DINO) to query the negated concept. For each frame, we obtain the maximum detection confidence score d_t for the negated object and report

$$\text{DINO-conf} = \frac{1}{T} \sum_{t=1}^T d_t.$$

Lower values indicate stronger suppression of the forbidden object category. This metric evaluates object-level compliance independently of embedding similarity.

Together, these metrics quantify (1) global prompt alignment, (2) negated concept suppression, and (3) object-level presence, providing a comprehensive yet standard evaluation of negation-aware video generation without introducing custom or threshold-dependent measures.

Vision-Language Negation Compliance Evaluation (NCS and NVR). While the preceding metrics quantify alignment and suppression within embedding or detection spaces, they do not directly measure whether negation constraints are semantically satisfied at the reasoning level. In particular, embedding-based metrics operate within representational spaces that may themselves underrepresent linguistic negation. Since our method explicitly targets negation-aware generation, evaluating compliance solely within CLIP similarity space may introduce circularity. To address this limitation, we introduce two complementary metrics based on a direct vision-language judge: the *Negation Compliance Score (NCS)* and the *Negation Violation Rate (NVR)*.

Evaluation Principle. Instead of comparing embeddings, we directly query a multimodal large language model (LLM) capable of joint visual and textual reasoning. The judge receives (i) the full original textual prompt P , including negation phrases (e.g., “no”, “without”, “not”), (ii) the extracted negated concept c_{neg} , obtained via rule-based parsing from the prompt, and (iii) multiple frames uniformly sampled from the generated video across its temporal span. The frames are resized with preserved aspect ratio to ensure consistent visual input resolution. No cropping, object masking, or post-processing is applied.

Judge Configuration. We use GPT-4o as a multimodal judge accessed through the OpenAI API. The model is instructed to evaluate *negation compliance only*, explicitly ignoring overall aesthetic quality unless it affects the ability to determine the presence or usage of forbidden concepts. The evaluation rubric is fixed and provided verbatim to the judge to ensure consistency. The model operates with deterministic decoding (temperature set to 0) to reduce stochastic variability.

Scoring Rubric. For each video, the judge assigns an integer score $s \in \{1, 2, 3, 4, 5\}$ defined as:

- 1: Clear violation (forbidden concept/action prominently present).
- 2: Likely violation (forbidden concept appears at least once with clear evidence).
- 3: Ambiguous or uncertain.
- 4: Mostly compliant (no clear forbidden evidence, minor uncertainty).
- 5: Fully compliant (strong evidence forbidden concept/action is absent).

In addition, the judge outputs a binary indicator `forbidden_present` indicating whether the forbidden concept/action is visually present or used in the video according to its reasoning.

Negation Compliance Score (NCS). Let s_i denote the integer compliance score assigned to video i among N evaluated samples. We define:

$$\text{NCS} = \frac{1}{N} \sum_{i=1}^N s_i.$$

NCS ranges from 1 to 5. Higher values indicate stronger semantic compliance with negation constraints.

Negation Violation Rate (NVR). Let v_i be defined as:

$$v_i = \begin{cases} 1 & \text{if } \text{forbidden_present}_i = \text{True}, \\ 0 & \text{otherwise.} \end{cases}$$

We define:

$$\text{NVR} = \frac{1}{N} \sum_{i=1}^N v_i.$$

NVR measures the empirical frequency of explicit negation violations across the evaluation set. Lower values indicate stronger suppression of forbidden concepts.

Aggregation Protocol. All NCS and NVR values are computed over the full evaluation set without thresholding, sample exclusion, or post-hoc correction. Ambiguous cases (score = 3) are retained in the computation. The binary violation indicator directly reflects the judge’s decision regarding forbidden presence, without manual reinterpretation.

Rationale. Unlike embedding-based metrics, NCS and NVR evaluate negation compliance through direct multimodal reasoning over visual evidence. This removes reliance on CLIP similarity space and avoids circular evaluation in representational embeddings. By combining embedding-based alignment metrics with direct vision-language compliance scoring, we obtain complementary measurements of semantic fidelity and constraint satisfaction.

Overall Performance. As shown in **Table 2**, our full model achieves the highest CLIPScore (0.2924 ± 0.0225), indicating improved global alignment with the complete textual prompt compared to all baselines. Importantly, this improvement in overall text-video alignment is achieved simultaneously with stronger negation suppression. Our method reduces CLIP-neg from 0.2411 ± 0.0288 (Mochi) to 0.2336 ± 0.0231 , corresponding to a relative reduction of approximately 3.1%.

Beyond embedding-based metrics, direct vision-language evaluation further confirms this trend. Our full model attains the highest Negation Compliance Score (NCS) of 4.0700 ± 1.6406 , outperforming Mochi (3.5789 ± 1.8548) and all other baselines. Simultaneously, it achieves the lowest Negation Violation Rate (NVR) of 0.2300 ± 0.4213 , representing a substantial reduction compared to Mochi (0.3625 ± 0.4813). These results indicate that negation-aware control improves both semantic fidelity and constraint compliance under direct multimodal reasoning.

The reported standard deviations reflect variability across diverse negation scenarios and video samples. Notably, our method exhibits consistently lower mean violation rates while maintaining competitive or reduced dispersion compared to baselines, suggesting stable negation suppression across the evaluation set.

Object-Level Suppression. The DINO detection confidence further corroborates these findings. Our method achieves the lowest DINO-conf score (0.0167 ± 0.0278), representing a 4.6% relative reduction compared to Mochi. This indicates that the repulsive guidance mechanism effectively suppresses the presence of forbidden objects at the detection level, independently of embedding similarity. Combined with the improvements in NCS and NVR, these results demonstrate that constraint scheduling and repulsive energy jointly enhance both object-level suppression and holistic semantic compliance.

Category-wise Negation Analysis. To further understand how different forms of linguistic negation affect generation behavior, we provide a **category-wise breakdown** of performance across the eight negation types introduced in our benchmark. **Table 3 reports CLIPScore, Negation Compliance Score (NCS), and Negation Violation Rate (NVR) for each category.**

This analysis reveals several important trends regarding the difficulty of different negation forms. First, the **INA** (Implicit Natural-only Constraint) category exhibits near-saturation behavior across all methods. In this setting, NCS values approach the maximum score while NVR remains near zero for most models. This indicates that implicit exclusivity expressed through constructions such as “only” is largely captured by the generative priors of pretrained diffusion models. Consequently, INA represents a relatively easier form of negation where even baseline models can satisfy the constraint without explicit suppression mechanisms.

In contrast, categories that require *explicit semantic suppression* or *compositional reasoning over negation* show substantially larger performance differences between methods. For instance, the **AOC** (Absence of Object Constraint) and **MNC** (Multi-object Negation Constraint) categories require models to actively suppress the appearance of one or more forbidden entities. In these settings, our method consistently achieves higher CLIPScore and NCS while reducing NVR compared to all baselines. Notably, in the MNC category our method improves NCS to 2.92 while reducing NVR to 0.52, demonstrating stronger control when multiple forbidden concepts must be simultaneously excluded.

More structurally complex negation forms further highlight the advantages of our approach. In the **SFN** (Structural Functional Negation) category, which involves suppressing objects based on functional relationships rather than simple presence, our model achieves a substantially higher NCS (4.68) while maintaining the lowest violation rate (0.10). This suggests that the proposed constraint formulation enables more precise suppression of semantically constrained entities.

The most challenging settings arise in categories involving *compositional negation reasoning*. In particular, the **DNS** (Double Negation Sensitivity) and **SND** (Scoped Negation Disambiguation) categories require resolving nested or scope-dependent negation structures. These cases are known to be difficult for both language and vision-language models. Nevertheless, our method achieves the strongest performance in both settings. For DNS, our model attains the highest NCS (4.92) while eliminating explicit violations ($\text{NVR} = 0$). Similarly, in the SND category our approach achieves perfect compliance ($\text{NCS} = 5.0, \text{NVR} = 0$), whereas competing methods continue to exhibit noticeable violation rates.

Overall, this category-wise analysis demonstrates that the benefits of our constraint-based formulation become increasingly pronounced as the linguistic complexity of negation increases. While simpler forms of negation (e.g., INA) are largely handled by pretrained generative priors, more challenging settings involving explicit suppression, multi-object exclusion, and compositional reasoning reveal substantial performance gaps. These results confirm that our approach primarily improves *difficult negation scenarios* rather than trivial cases, highlighting the importance of structured constraint guidance for reliable negation-aware generation.

Category	Method	CLIPScore \uparrow	NCS \uparrow	NVR \downarrow
AOC	Mochi	0.2878	2.2800	0.6800
	HunyuanVideo	0.2735	1.7200	0.8200
	CogVideoX	0.2805	2.3200	0.6800
	Ours	0.2967	2.4600	0.6400
LEN	Mochi	0.2886	3.3200	0.5000
	HunyuanVideo	0.2858	2.5800	0.6200
	CogVideoX	0.2878	2.7800	0.5600
	Ours	0.2931	3.1200	0.4800
INA	Mochi	0.2939	5.0000	0.0000
	HunyuanVideo	0.2935	5.0000	0.0000
	CogVideoX	0.2935	4.9600	0.0000
	Ours	0.3010	5.0000	0.0000
MNC	Mochi	0.2852	1.4600	0.9000
	HunyuanVideo	0.2844	1.1800	0.9600
	CogVideoX	0.2814	1.9000	0.7800
	Ours	0.2948	2.9200	0.5200
SFN	Mochi	0.2908	3.8800	0.3000
	HunyuanVideo	0.2740	3.6800	0.2800
	CogVideoX	0.2846	3.4400	0.3600
	Ours	0.2922	4.6800	0.1000
NMI	Mochi	0.2746	4.3265	0.1400
	HunyuanVideo	0.2498	3.3877	0.3200
	CogVideoX	0.2739	4.1489	0.1800
	Ours	0.2806	4.4600	0.1000
DNS	Mochi	0.2765	4.4600	0.1000
	HunyuanVideo	0.2585	3.5200	0.2800
	CogVideoX	0.2767	4.0200	0.2000
	Ours	0.2858	4.9200	0.0000
SND	Mochi	0.2916	3.9200	0.2800
	HunyuanVideo	0.2753	3.5600	0.2400
	CogVideoX	0.2903	3.7400	0.2800
	Ours	0.2951	5.0000	0.0000

Table 3. **Category-wise quantitative evaluation across eight negation types.** We report CLIPScore (\uparrow), Negation Compliance Score (NCS, \uparrow), and Negation Violation Rate (NVR, \downarrow) for each negation category. While simple implicit negation (INA) shows near-saturation performance across models, more complex forms of negation such as MNC, SFN, DNS, and SND reveal substantial performance gaps, where our method consistently achieves higher compliance and lower violation rates.

E. Detailed Ablation Study

We validate the contributions of our two core components: the *Repulsive CLIP Energy* and *Constraint Scheduling*. The repulsive term operationalizes negation as a geometric constraint in guidance space, while scheduling governs its temporal activation along the diffusion trajectory. These modules respectively determine *which semantic direction is restricted* and *when the restriction becomes active*.

Effect of Removing Repulsive Energy. In “Ours w/o Repulsive Energy,” we retain the original prompt (including its negation phrasing) and preserve the same diffusion backbone and CFG structure. However, we disable the negation-specific control pathway: the auxiliary negated-component branch is not constructed, the semantic negation direction a_t is not formed, and no feasibility projection is applied to the reference guidance increment. The denoising update therefore proceeds without geometric restriction in guidance space, eliminating structured negation control while leaving global semantic conditioning unchanged. As shown in **Table 2**, removing the projection-based repulsive mechanism increases CLIP-neg from $0.2336 \pm$

Criterion	Ours	w/o Repulsive	w/o Scheduling
Negation Satisfaction	5.00 ± 0.00	2.90 ± 1.94	2.90 ± 1.94
Constraint Meaning Accuracy	5.00 ± 0.00	2.70 ± 1.75	2.40 ± 1.58
Scene & Action Alignment	5.00 ± 0.00	3.00 ± 2.02	2.90 ± 1.94
Artifact Avoidance	5.00 ± 0.00	2.60 ± 1.70	1.90 ± 1.59

Table 4. **Human perceptual ablation study** Participants compared the full model with two ablation variants. The full model consistently achieved the highest ratings across all perceptual criteria.

0.0231 to 0.2411 ± 0.0281 , effectively reverting to baseline-level negation suppression. Importantly, CLIPScore remains statistically unchanged (0.2924 ± 0.0225 vs. 0.2924 ± 0.0221), indicating that global alignment fidelity is preserved even as negation compliance deteriorates. This separation confirms that suppression of forbidden semantics does not arise from incidental prompt alignment but from explicit feasibility enforcement in semantic guidance space. The degradation becomes clearer under direct vision-language evaluation. NCS decreases from 4.0700 ± 1.6406 to 3.9548 ± 1.6724 , while NVR increases from 0.2300 ± 0.4213 to 0.2625 ± 0.4405 . Both the mean violation rate and its variance increase, demonstrating that without projection, suppression becomes unstable across negation categories. DINO-conf similarly rises from 0.0167 ± 0.0278 to 0.0181 ± 0.0301 , reflecting weakened object-level exclusion. These results indicate that negation compliance is not an emergent property of CFG dynamics, but a consequence of explicit geometric constraint.

Effect of Removing Constraint Scheduling. In “Ours w/o Constraint Scheduling,” the repulsive projection remains active, but its strength is no longer temporally modulated. The constraint is applied uniformly across diffusion timesteps, removing progressive tightening. While negation directionality is preserved, its interaction with structural formation becomes unregulated. Quantitatively, CLIPScore drops from 0.2924 ± 0.0225 to 0.2800 ± 0.0305 , and BLIP decreases from 0.8201 ± 0.0729 to 0.7869 ± 0.0881 , indicating reduced global fidelity. CLIP-neg increases to 0.2405 ± 0.0477 , reflecting unstable suppression magnitude. Under direct compliance metrics, NCS falls to 3.5789 ± 1.8439 and NVR rises to 0.3625 ± 0.4813 , showing both mean degradation and higher dispersion. This confirms that temporal scheduling is critical for balancing early structural coherence with late-stage semantic enforcement.

Qualitative analysis. Figure 4 illustrates complementary failure modes. Without projection, forbidden semantics intermittently reappear, producing temporal artifacts such as lighting flicker under DNS. Without scheduling, negation constraints interfere with early structural stabilization, causing scale drift and unnatural lighting geometry. The full model maintains geometric stability while satisfying double-negation constraints, demonstrating coordinated control across semantic and temporal dimensions. Overall, the ablation study clarifies that performance gains arise from structured convex feasibility enforcement rather than heuristic prompt manipulation. The repulsive projection establishes principled semantic exclusion, while scheduling ensures stable integration within diffusion dynamics. Both are necessary for achieving robust negation compliance without sacrificing global prompt fidelity.

Human Perceptual Ablation. To complement the quantitative ablation analysis, we additionally conducted a small human evaluation comparing the full model against two ablation variants. In this task (Q9), participants evaluated three anonymized videos corresponding to *Ours*, *Ours w/o Repulsive Energy*, and *Ours w/o Constraint Scheduling*. As summarized in Table 4, the full model consistently received the highest ratings across all perceptual criteria. Notably, the complete model achieved perfect mean scores (5.00) across all four evaluation axes, while both ablation variants exhibited substantial degradation. In the overall preference selection, **100% of participants selected the full model**. These results confirm that the improvements observed in quantitative metrics also translate to human perceptual evaluation, further validating the necessity of both the repulsive projection mechanism and temporal constraint scheduling.

F. Detailed User Study

Motivation. While automated metrics such as NCS and NVR provide quantitative evidence of negation compliance, they rely on GPT-based evaluators, which may themselves exhibit limitations in linguistic negation understanding. This introduces a potential circularity concern when GPT models are used both as generators and judges. To mitigate this concern and validate metric reliability, we conducted a human evaluation study to directly assess perceptual quality and semantic compliance.

The user study serves two purposes: (1) to provide independent human validation of negation-aware generation quality, and (2) to examine whether improvements observed in automated metrics correlate with human judgment.

Participants. The study involved **50 participants**. Participants were adults (18 years or older) recruited through open online channels and academic mailing lists. They represent a general technical audience rather than a domain-specific expert group in diffusion modeling. No prior expertise in generative video models was required. Participants were not affiliated with this project, and no personally identifiable information was collected. All responses were anonymized prior to analysis.

IRB and Ethical Considerations. The study consisted of a short (10–15 minute) anonymous survey involving perceptual comparison of AI-generated videos. No sensitive data were collected, and participants received no monetary compensation. The study protocol was reviewed by the Institutional Review Board (IRB) at University of Maryland (Kuali-IRB Number #1179-1) and determined to be exempt (45 CFR Part 46 - Protection of Human Subjects) under minimal-risk research guidelines.

Protocol. Each participant evaluated 8 evaluation tasks (Q1–Q8). The human study was restricted to 8 evaluation tasks, one per negation category, due to IRB constraints on survey duration and participant burden. The selected prompts were randomly sampled from the evaluation set while ensuring coverage of diverse negation types (e.g., object absence, logical exclusion, and scoped negation). This subset was designed to be representative rather than exhaustive, enabling controlled human comparison under limited survey time. For every prompt, four anonymized videos (Mochi, HunyuanVideo, CogVideoX, and *Ours*) were shown simultaneously. In addition, participants evaluated one supplementary task (Q9) designed to compare the ablated variants of our method. This task presents results from *Ours*, *Ours w/o Repulsive Energy*, and *Ours w/o Constraint Scheduling* to examine perceptual differences associated with the proposed components. Detailed descriptions of this ablation-focused evaluation are provided in Appendix E.

To prevent positional bias:

- The mapping between models and labels (Video A–D) was randomized across questions.
- The presentation order of videos was shuffled per question.
- Model identities were fully anonymized.

Each participant rated every video on four criteria using a 5-point Likert scale:

1. **Negation Satisfaction**
2. **Constraint Meaning Accuracy**
3. **Scene & Action Alignment**
4. **Artifact Avoidance**

Participants also selected one overall preferred video per question.

Across 50 participants and 8 evaluation tasks, each model received **400 ratings per criterion**.

Overall Preference. As summarized in Table 5, our method consistently achieved the highest ratings across all evaluation criteria. Out of **400 total votes**, *Ours* was selected in **77.5%** of cases (95% CI [0.73, 0.82]), compared to 13.8% for HunyuanVideo, 8.8% for Mochi, and 0.0% for CogVideoX.

Human–Metric Consistency. The strong human preference for *Ours* aligns with the improvements observed in automated metrics (NCS and NVR), indicating that these metrics meaningfully correlate with human perception of negation compliance. The user study therefore serves as an external validation of metric reliability, mitigating concerns regarding potential circularity when GPT-based evaluators are used.

G. Computation Time and Memory Consumption

Table 6 summarizes peak GPU memory consumption and end-to-end inference time measured on a single NVIDIA H100 (80GB). Overall, our full method (**Ours**) uses 28.26 GB and takes 235 sec per inference, which is comparable in memory to modern diffusion-based baselines, while incurring additional runtime due to the proposed constraint-control components.

Criterion	Model	Mean	Std	95% CI
Negation Satisfaction	Ours	4.76	0.88	[4.68, 4.85]
	Mochi	1.96	1.56	[1.81, 2.12]
	HunyuanVideo	1.61	1.32	[1.48, 1.74]
	CogVideoX	1.34	0.84	[1.26, 1.42]
Constraint Meaning Accuracy	Ours	4.75	0.89	[4.66, 4.84]
	Mochi	1.94	1.52	[1.79, 2.09]
	HunyuanVideo	1.58	1.20	[1.46, 1.69]
	CogVideoX	1.36	0.73	[1.29, 1.43]
Scene & Action Alignment	Ours	4.84	0.37	[4.80, 4.87]
	Mochi	2.64	1.82	[2.46, 2.82]
	HunyuanVideo	2.75	1.85	[2.57, 2.93]
	CogVideoX	2.34	1.61	[2.18, 2.50]
Artifact Avoidance	Ours	4.54	0.91	[4.45, 4.63]
	Mochi	1.94	1.43	[1.80, 2.08]
	HunyuanVideo	2.83	1.86	[2.64, 3.01]
	CogVideoX	1.80	1.24	[1.68, 1.92]

Table 5. **Human evaluation results (50 participants, 400 ratings per model per criterion)**. Our method consistently achieves the highest mean scores across all evaluation criteria with strong inter-participant agreement.

Model	Step	Memory Consumption	Computation Time
Ours	Inference	28.2580 GB / 80.0000 GB (26,949 MiB)	235 sec
Ours w/o Repulsive Energy	Inference	25.2843 GB / 80.0000 GB (24,113 MiB)	117 sec
Ours w/o Constraint Scheduling	Inference	28.2496 GB / 80.0000 GB (26,941 MiB)	168 sec
Mochi	Inference	26.2406 GB / 80.0000 GB (25,025 MiB)	114 sec
HunyuanVideo	Inference	41.3589 GB / 80.0000 GB (39,443 MiB)	396 sec
CogVideoX	Inference	16.7845 GB / 80.0000 GB (16,007 MiB)	61 sec

Table 6. **Inference-time memory consumption and runtime on NVIDIA H100 (80GB)**. We report peak GPU memory usage and end-to-end inference time for our full method and its ablations, together with three strong T2V baselines. Our full method (**Ours**) consumes 28.26 GB and requires 235 sec per inference. Removing the repulsive energy term reduces both memory and runtime to 25.28 GB and 117 sec, respectively. Removing constraint scheduling keeps memory nearly unchanged (28.25 GB) while reducing runtime to 168 sec. Among the baselines, HunyuanVideo shows the largest footprint (41.36 GB, 396 sec), whereas CogVideoX is the most lightweight and fastest (16.78 GB, 61 sec). All measurements are conducted under the same hardware setting (single NVIDIA H100 80GB GPU) and identical evaluation protocol.

Effect of the repulsive energy term. Comparing **Ours** against *Ours w/o Repulsive Energy*, we observe a clear increase in both memory and runtime when the repulsive energy is enabled. Specifically, the repulsive term adds +2.97 GB peak memory (25.28→28.26 GB, +11.7%) and +118 sec runtime (117→235 sec, +100.9%). This overhead is expected because the repulsive energy introduces additional similarity/energy evaluations and gradient-like guidance computations during denoising, which increases per-step compute and intermediate activation storage.

Effect of constraint scheduling. Comparing **Ours** with *Ours w/o Constraint Scheduling*, peak memory remains essentially unchanged (28.25 vs. 28.26 GB; < 0.05% difference), while runtime decreases substantially (168 vs. 235 sec; -67 sec, -28.5%). This indicates that scheduling primarily affects *how long* the constraints are actively enforced across timesteps (thereby changing total compute), rather than changing model size or the dominant activation footprint. In other words, scheduling is an effective mechanism to reduce runtime without sacrificing the memory budget.

Comparison to state-of-the-art T2V baselines. Among baselines, **Mochi** exhibits similar memory consumption to our method (26.24 GB) but is notably faster (114 sec), reflecting a lighter inference pathway without explicit constraint-control computations. **HunyuanVideo** shows the largest resource usage, requiring 41.36 GB and 396 sec, which is +13.10 GB (+46.4%) more memory and +161 sec (+68.5%) more time than **Ours**. **CogVideoX** is the most efficient, using 16.78 GB and 61 sec, i.e., -11.47 GB (-40.6%) less memory and -174 sec (-74.0%) less time than **Ours**. These results highlight that our approach targets improved *negation compliance* through inference-time control, and the compute overhead is the trade-off for enforcing repulsive constraints and their scheduling.

Takeaway. The two ablations reveal complementary roles: the repulsive energy term is the primary contributor to additional compute and memory, whereas constraint scheduling provides a practical knob that reduces runtime by 28.5% with virtually no memory change. This supports our design choice of coupling energy-based constraints with scheduling to manage the efficiency-control trade-off under a fixed GPU memory budget.

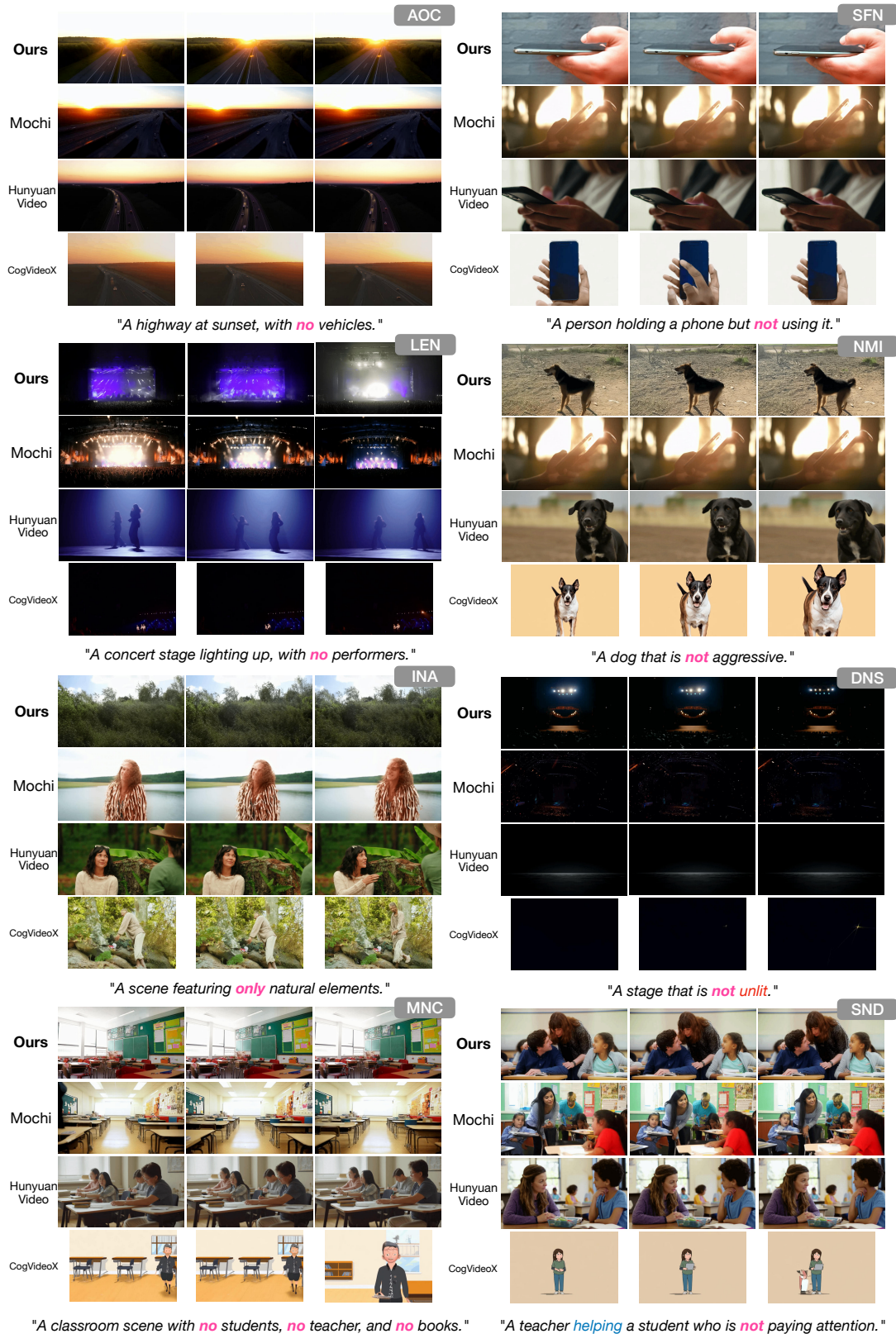


Figure 6. **Qualitative comparison across diverse negation scenarios.** We evaluate our model against state-of-the-art diffusion models (Mochi, HunyuanVideo, CogVideoX) on eight negation settings: AOC (Absent Object Consistency), LEN (Late Emergence Negation), INA (Implicit Natural-Only Attribute), MNC (Multi-Negation Composition), SFN (Structural Functional Negation), NMI (Non-Inversion Mitigation), DNS (Double Negation Sensitivity), and SND (Scoped Negation Disambiguation). Across simple object removal, functional suppression, logical inversion, and scope resolution, our model consistently preserves scene structure while correctly enforcing negation constraints.

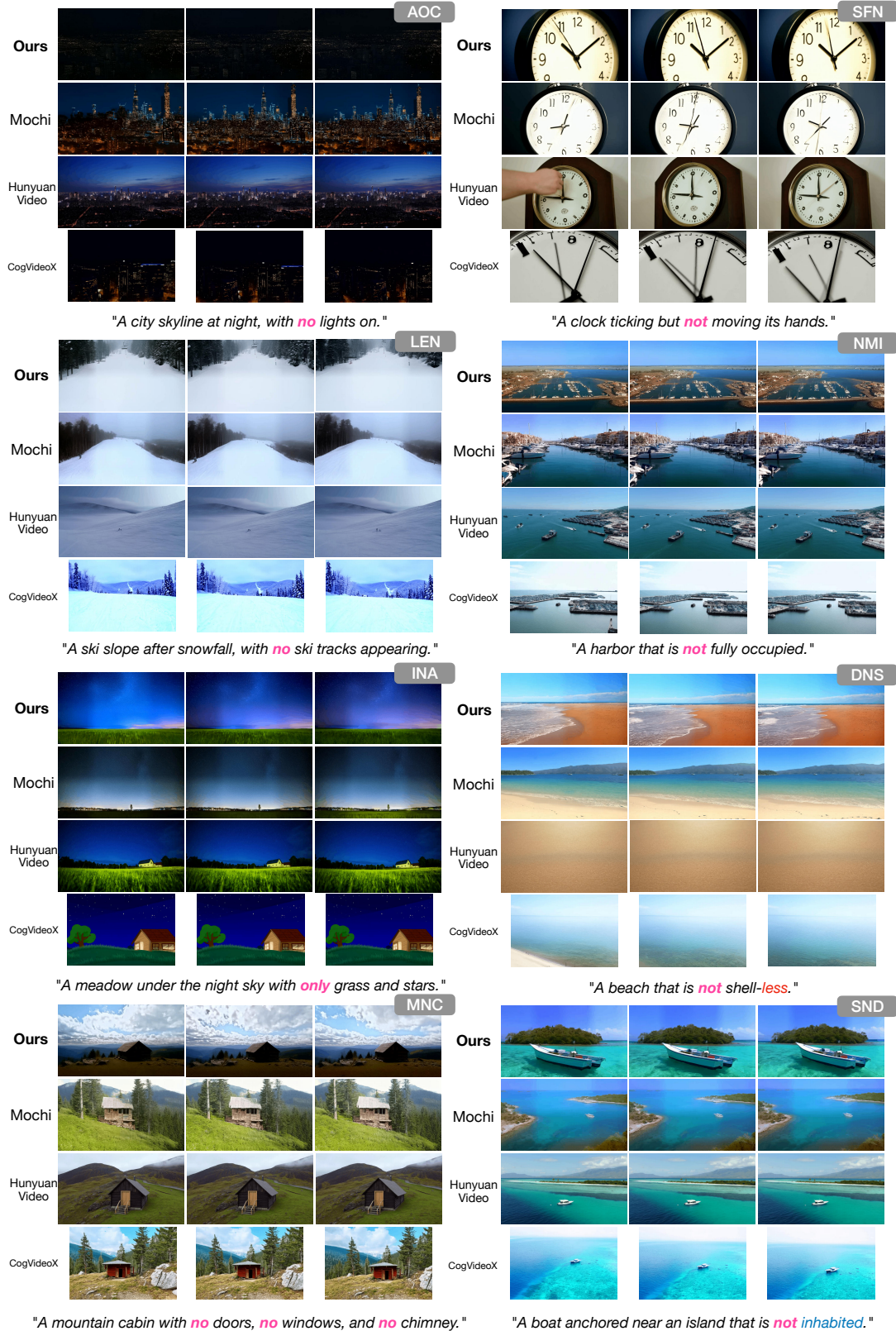


Figure 7. **Additional qualitative comparisons across diverse negation scenarios (Set 1).** We further evaluate our method against state-of-the-art diffusion-based video generation models (Mochi, HunyuanVideo, CogVideoX) on eight negation categories: AOC (Absent Object Consistency), LEN (Late Emergence Negation), INA (Implicit Natural-Only Attribute), MNC (Multi-Negation Composition), SFN (Structural Functional Negation), NMI (Non-Inversion Mitigation), DNS (Double Negation Sensitivity), and SND (Scoped Negation Disambiguation). Each row corresponds to a distinct negation prompt requiring suppression of objects, attributes, or functional behaviors while preserving the overall scene structure. Compared to competing methods, our approach consistently maintains semantic coherence while correctly enforcing the specified negation constraints across diverse environments and scene compositions.

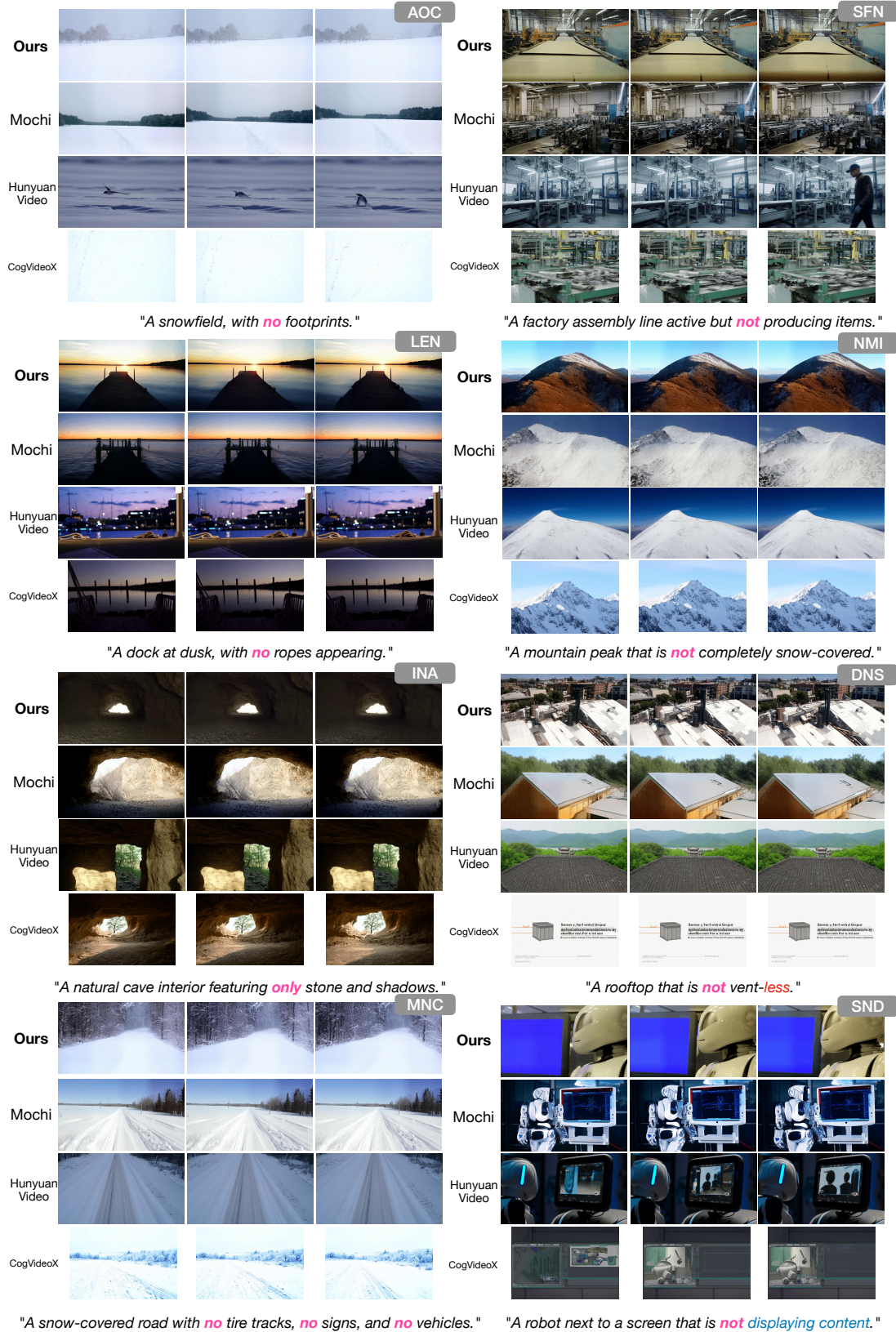
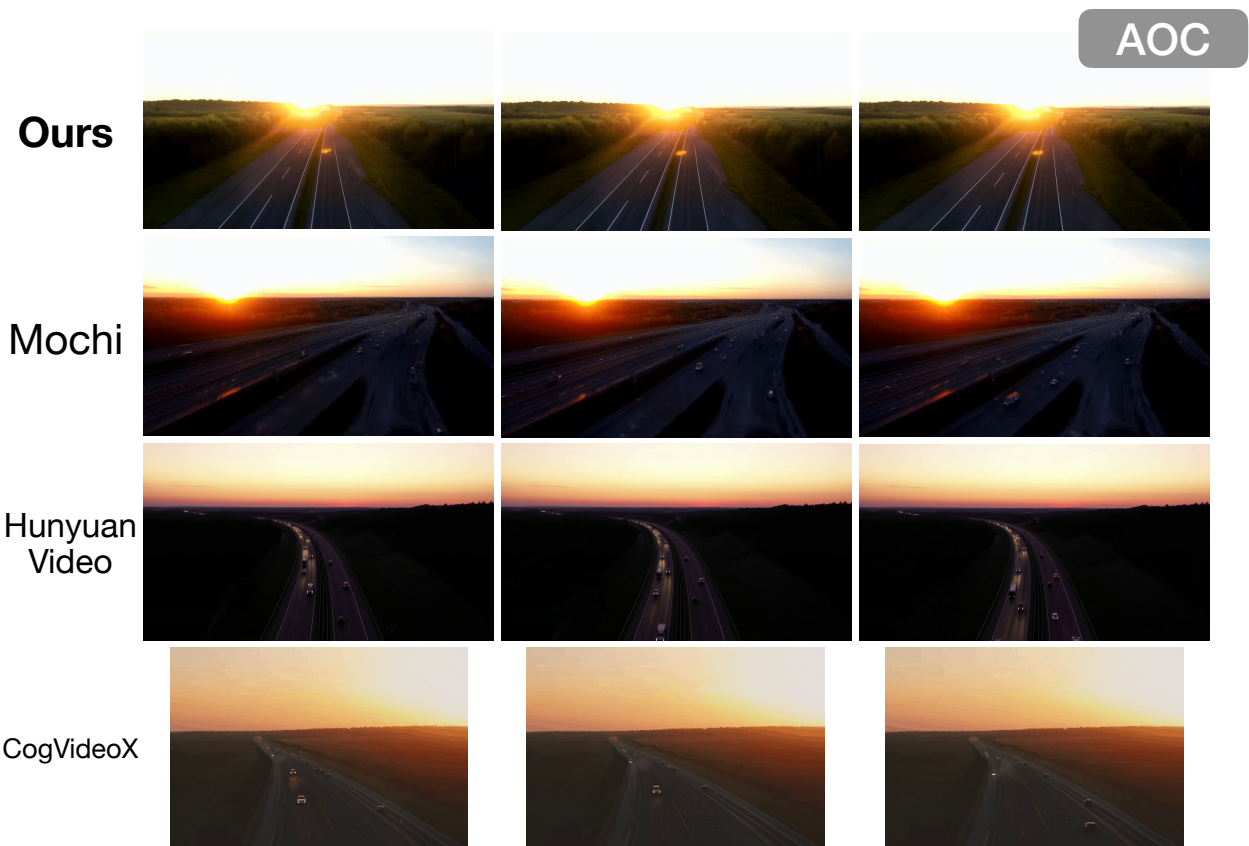
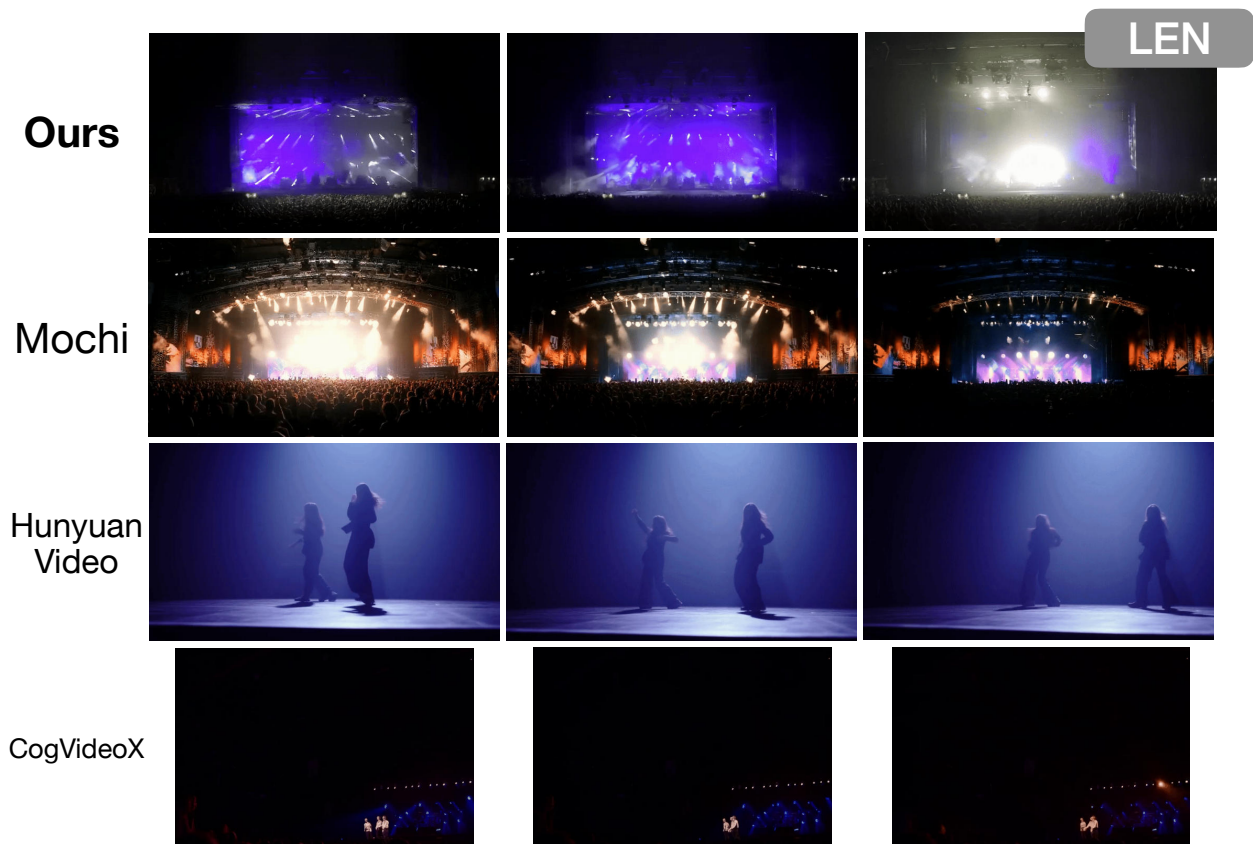


Figure 8. **Additional qualitative comparisons across diverse negation scenarios (Set 2).** This figure presents a second set of prompts covering the same eight negation categories as in Figure 6, including AOC, LEN, INA, MNC, SFN, NMI, DNS, and SND. These examples further highlight the robustness of our method across different scene contexts, ranging from natural landscapes and urban environments to structured indoor scenes and human-object interactions. While baseline models frequently violate negation constraints by introducing forbidden objects or attributes, our method reliably suppresses such elements while preserving scene realism and structural consistency.



*"A highway at sunset, with **no** vehicles."*

Figure 9. Comparison of negation compliance under the AOC (Absence of Object) scenario. Prompt: "A highway at sunset, with no vehicles." Our model removes the forbidden object while preserving global scene structure and lighting consistency, whereas competing diffusion models introduce unintended vehicles.



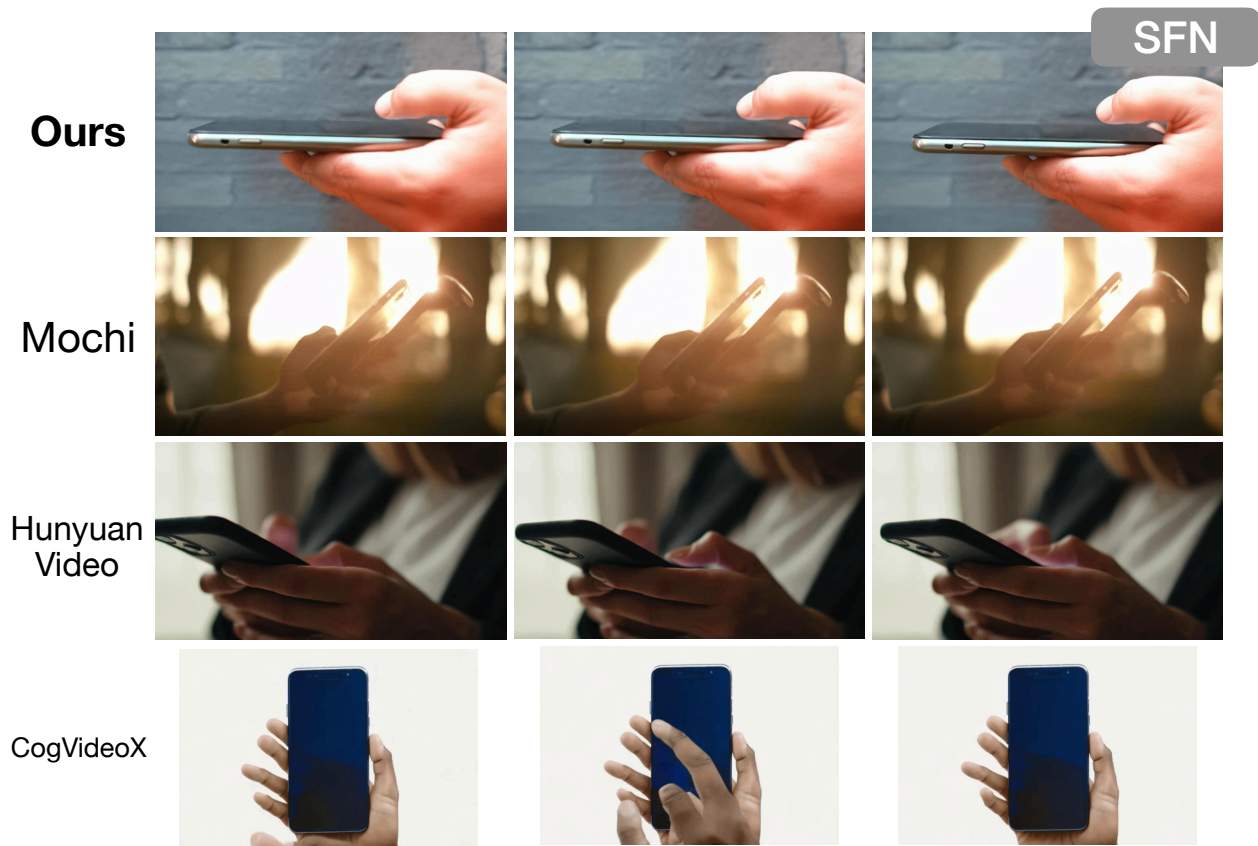
*"A concert stage lighting up, with **no** performers."*

Figure 10. Comparison of negation compliance under the LENS (Late Emergence Negation) scenario. Prompt: "A concert stage lighting up, with no performers." Our model enforces entity-level exclusion while maintaining realistic stage illumination, whereas baselines often hallucinate performers.



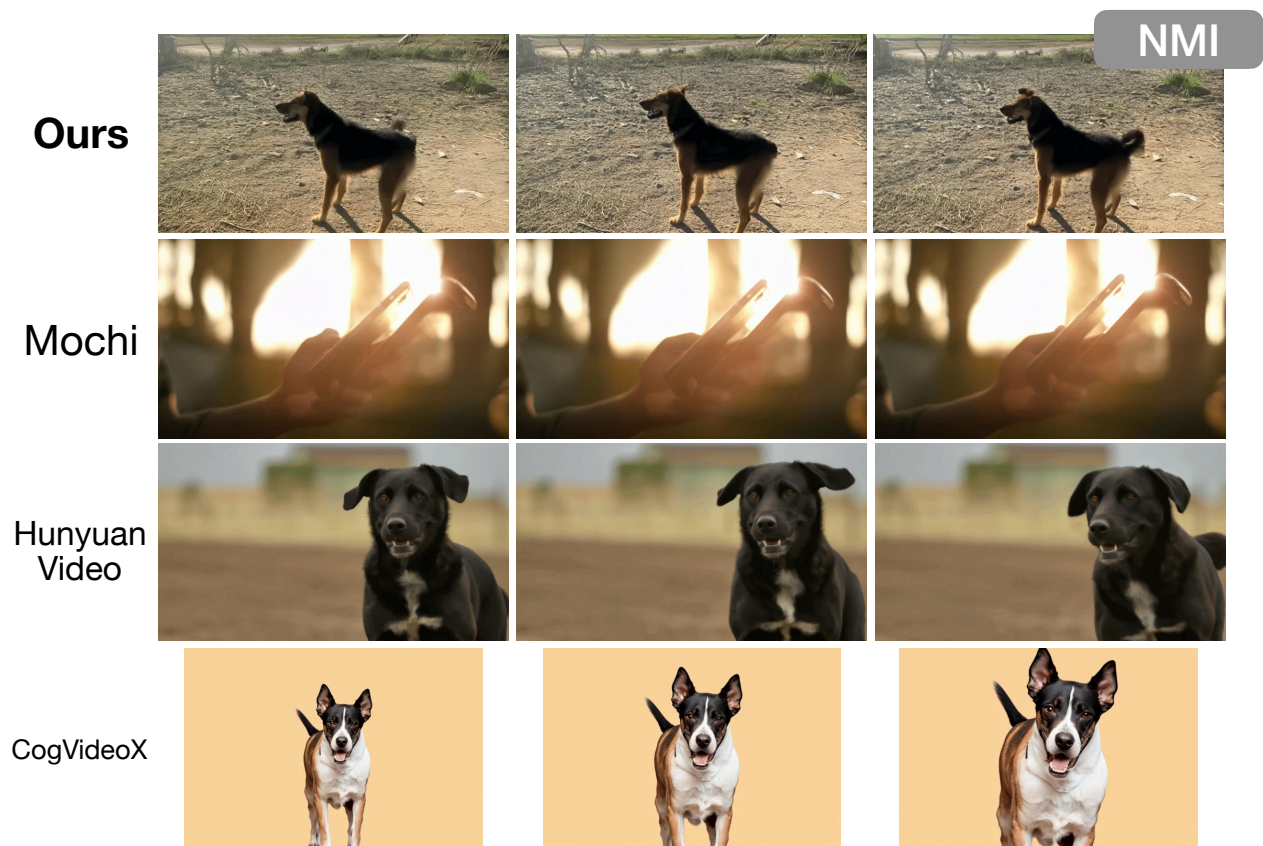
"A scene featuring *only* natural elements."

Figure 11. Comparison of negation compliance under the INA (Implicit Natural-Only Attribute) scenario. Prompt: "A scene featuring only natural elements." Our model suppresses human presence while preserving ecological coherence, unlike competing methods that introduce artificial objects.



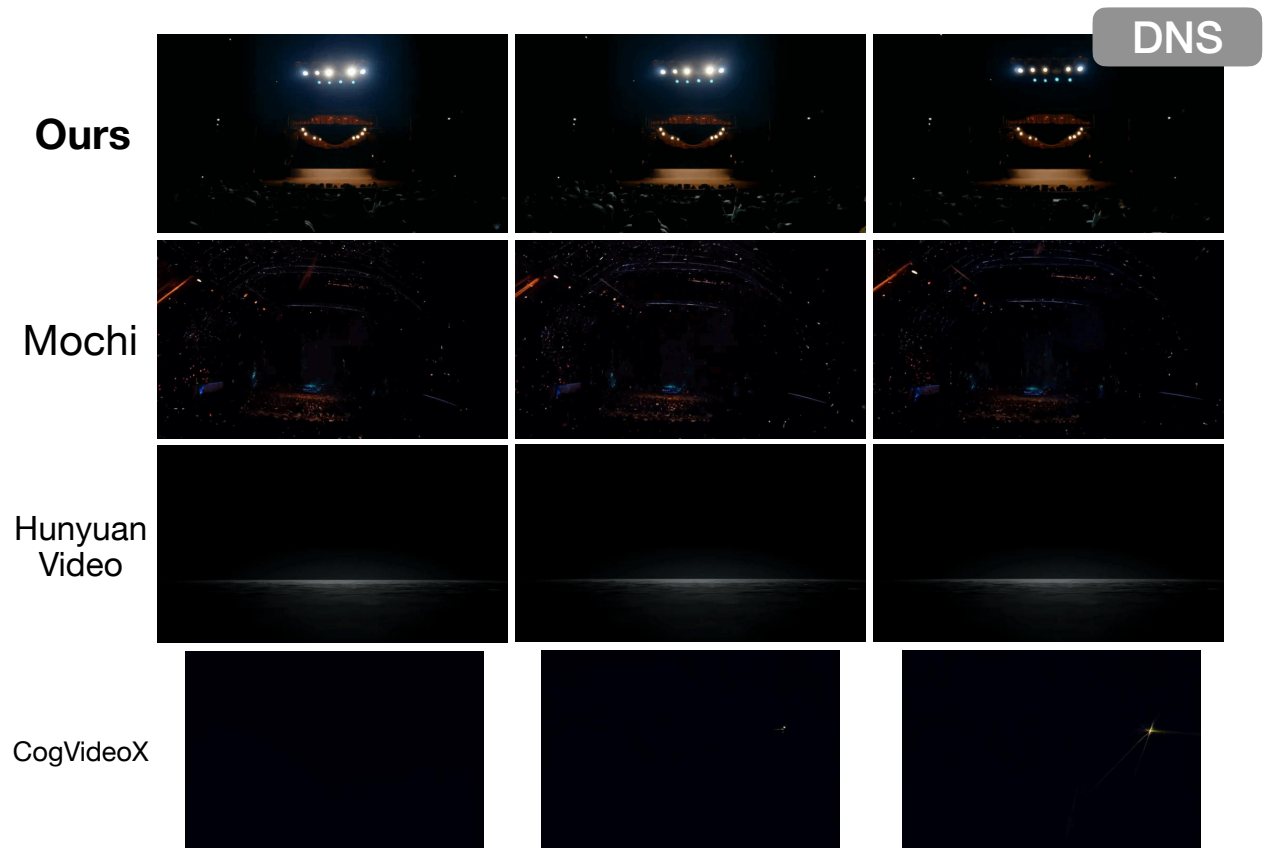
*"A person holding a phone but **not** using it."*

Figure 13. **Comparison of negation compliance under the SFN (Structural Functional Negation) scenario.** Prompt: "A person holding a phone but not using it." Our model suppresses the functional interaction while preserving object presence, whereas baselines conflate object existence with usage.



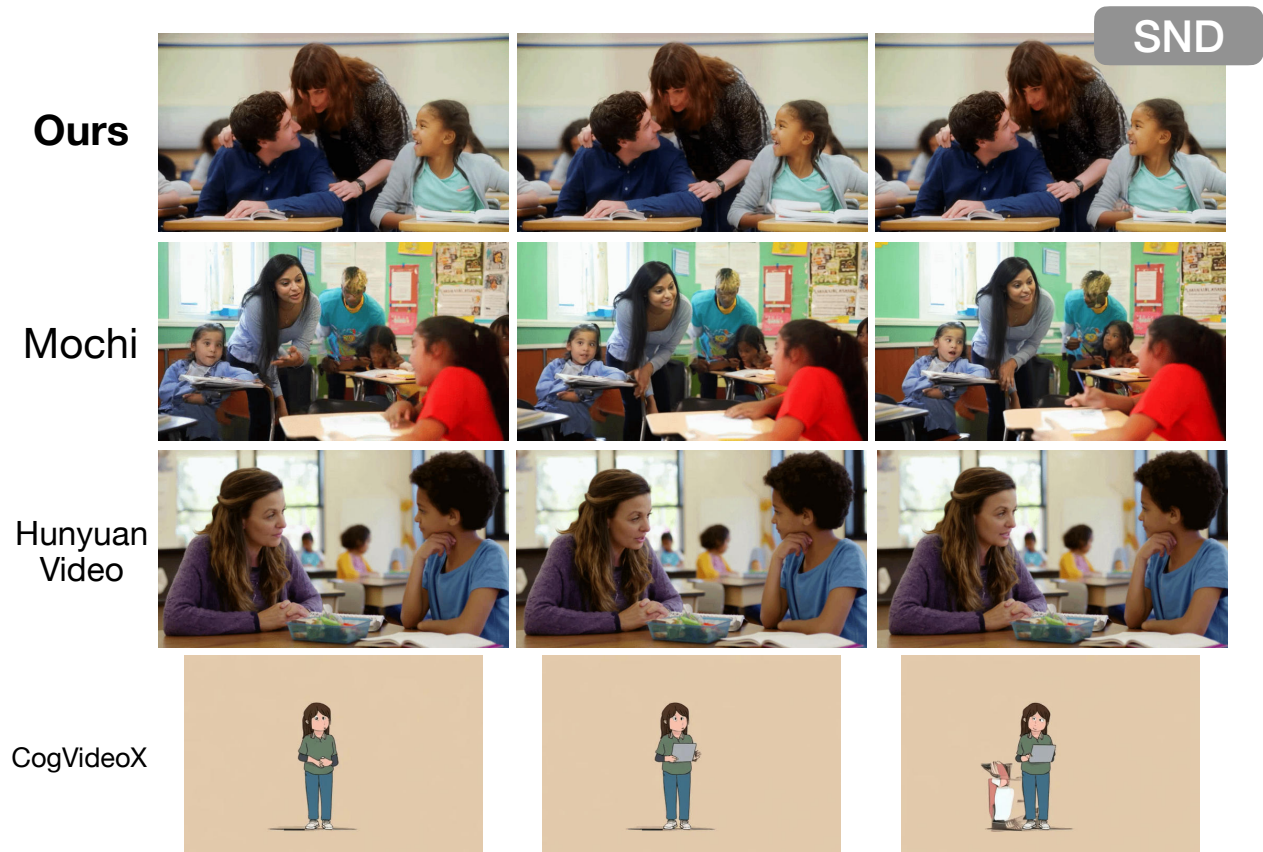
"A dog that is *not* aggressive."

Figure 14. Comparison of negation compliance under the NMI (Non-Inversion Mitigation) scenario. Prompt: "A dog that is not aggressive." Our model modulates behavioral attributes while maintaining subject identity, whereas competing models fail to disentangle appearance from disposition.



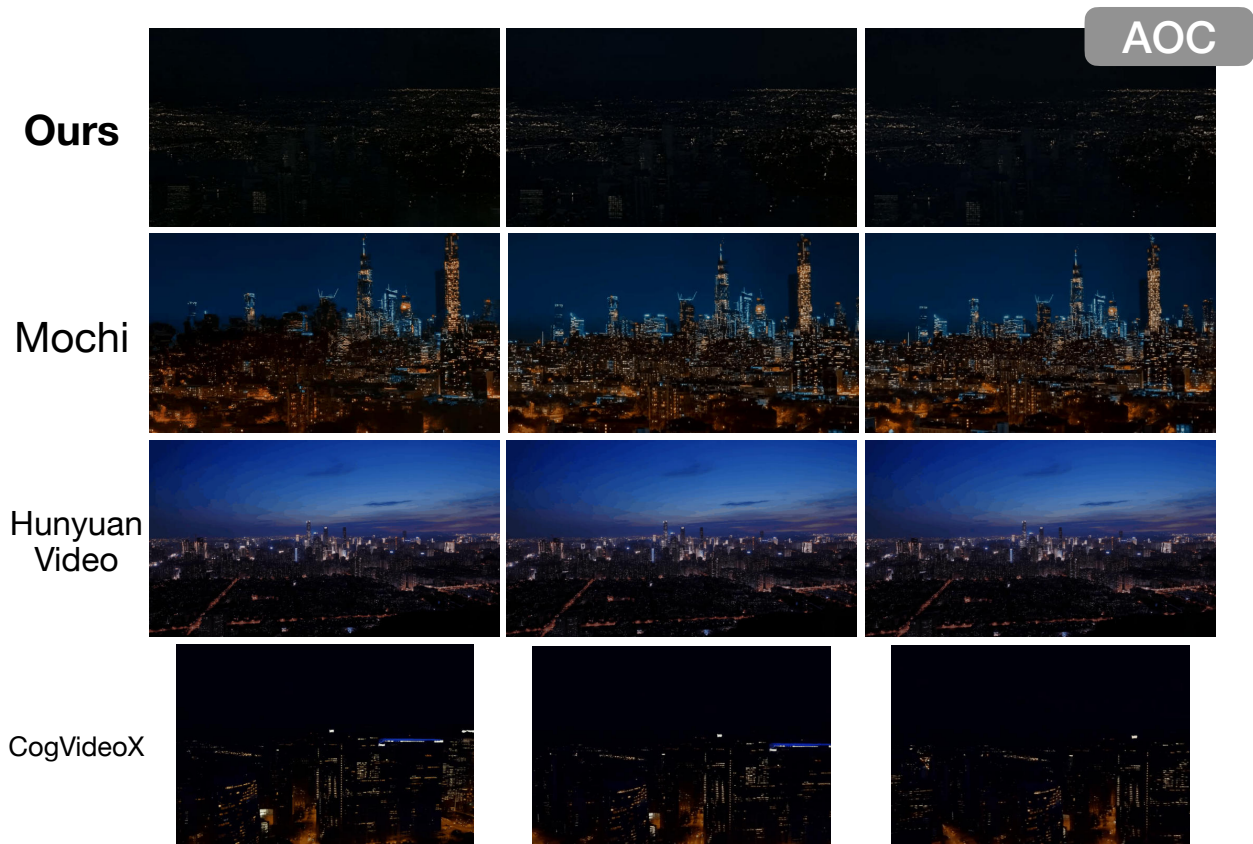
"A stage that is *not unlit*."

Figure 15. Comparison of negation compliance under the DNS (Double Negation Sensitivity) scenario. Prompt: "A stage that is not unlit." Our model correctly resolves double negation semantics, producing illuminated scenes, while baselines collapse into dark or ambiguous outputs.



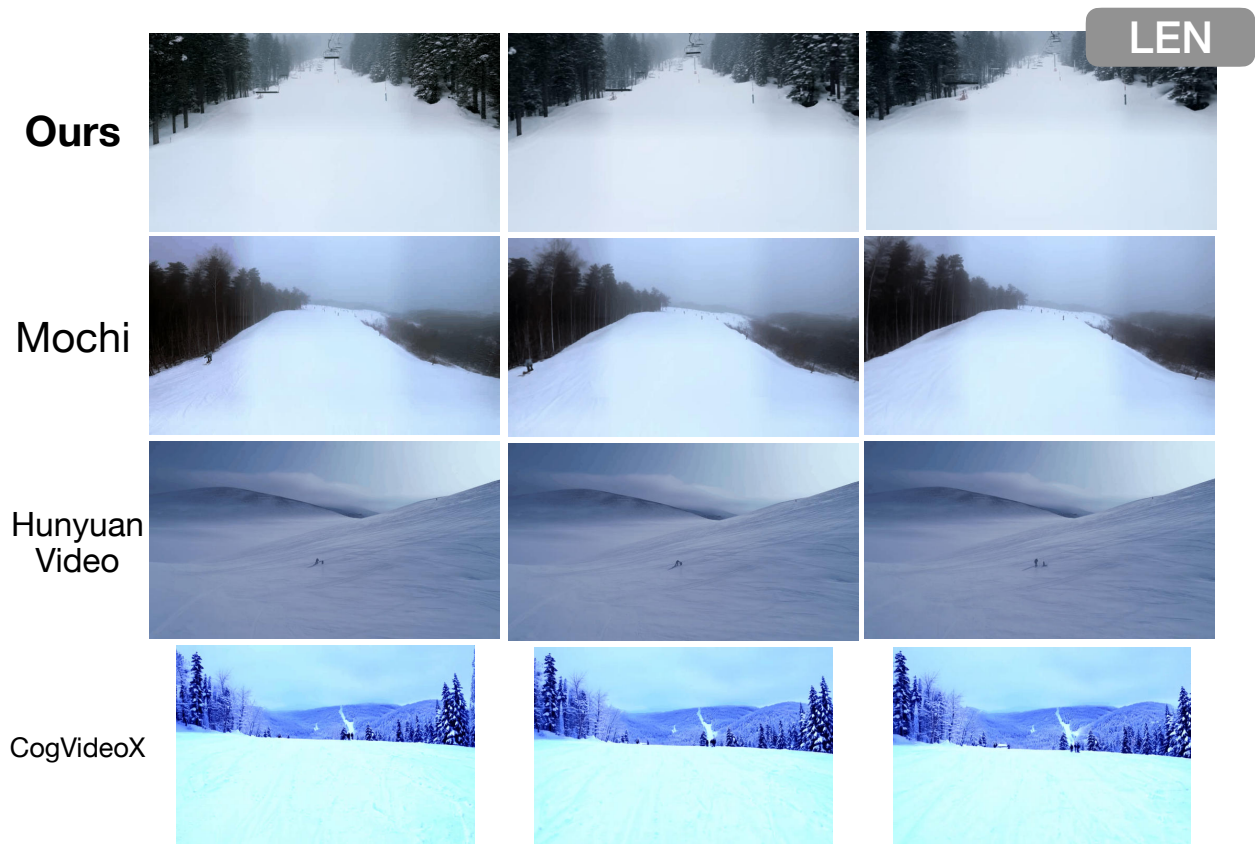
"A teacher *helping* a student who is *not* paying attention."

Figure 16. Comparison of negation compliance under the SND (Scoped Negation Disambiguation) scenario. Prompt: "A teacher helping a student who is not paying attention." Our model correctly localizes the negation scope to the student's behavior, whereas competing methods misinterpret the scope or alter unrelated elements.



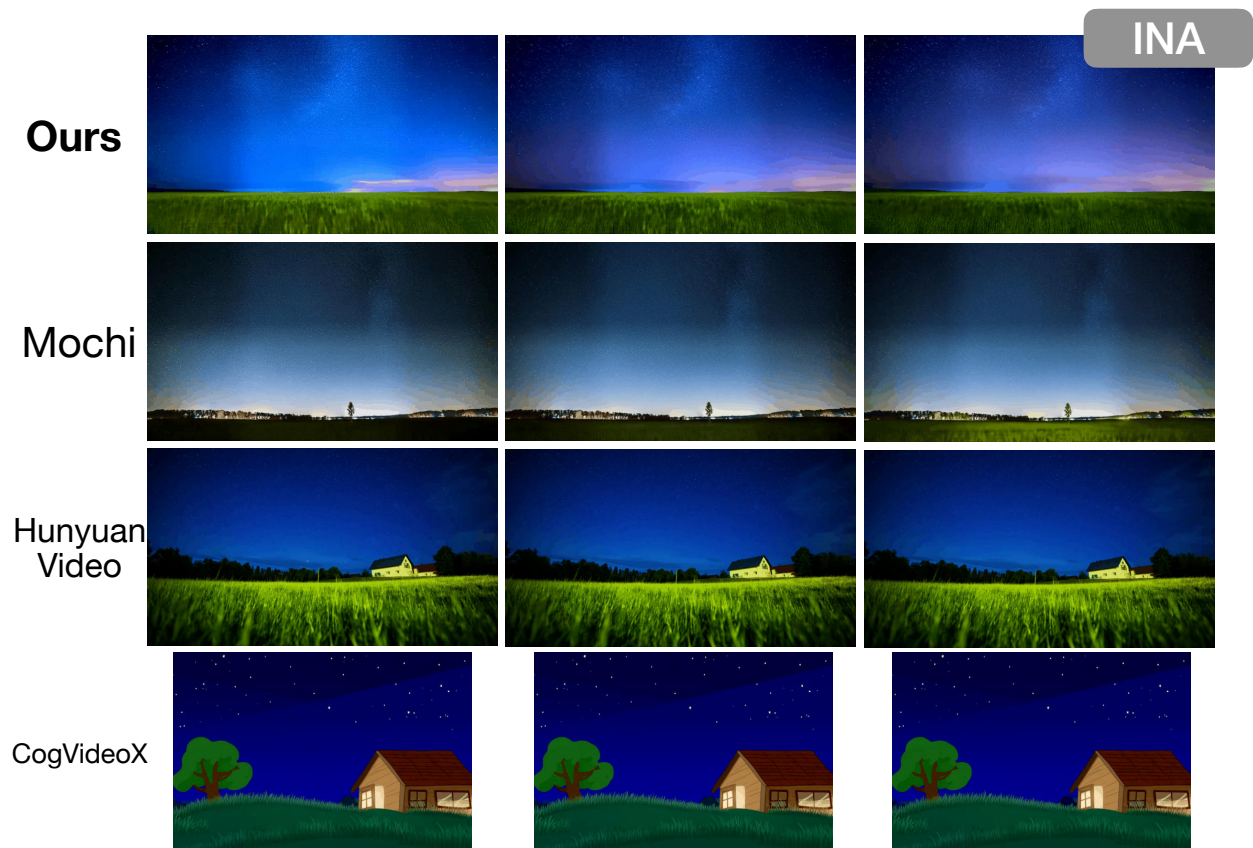
*"A city skyline at night, with **no** lights on."*

Figure 17. **Qualitative comparison under the AOC (Absence of Object) scenario.** Prompt: "A city skyline at night, with no lights on." Our model correctly suppresses artificial light sources across the skyline while preserving realistic nighttime structure. In contrast, Mochi and HunyuanVideo illuminate buildings despite the negation constraint, while CogVideoX produces unstable or partially lit scenes.



*"A ski slope after snowfall, with **no** ski tracks appearing."*

Figure 18. **Qualitative comparison under the LEN (Logical Exclusion of Entities) scenario.** Prompt: "A ski slope after snowfall, with no ski tracks appearing." Our model maintains a pristine snow surface consistent with the negation constraint. Competing models frequently introduce ski tracks or surface disturbances, indicating failure to enforce logical exclusion during generation.



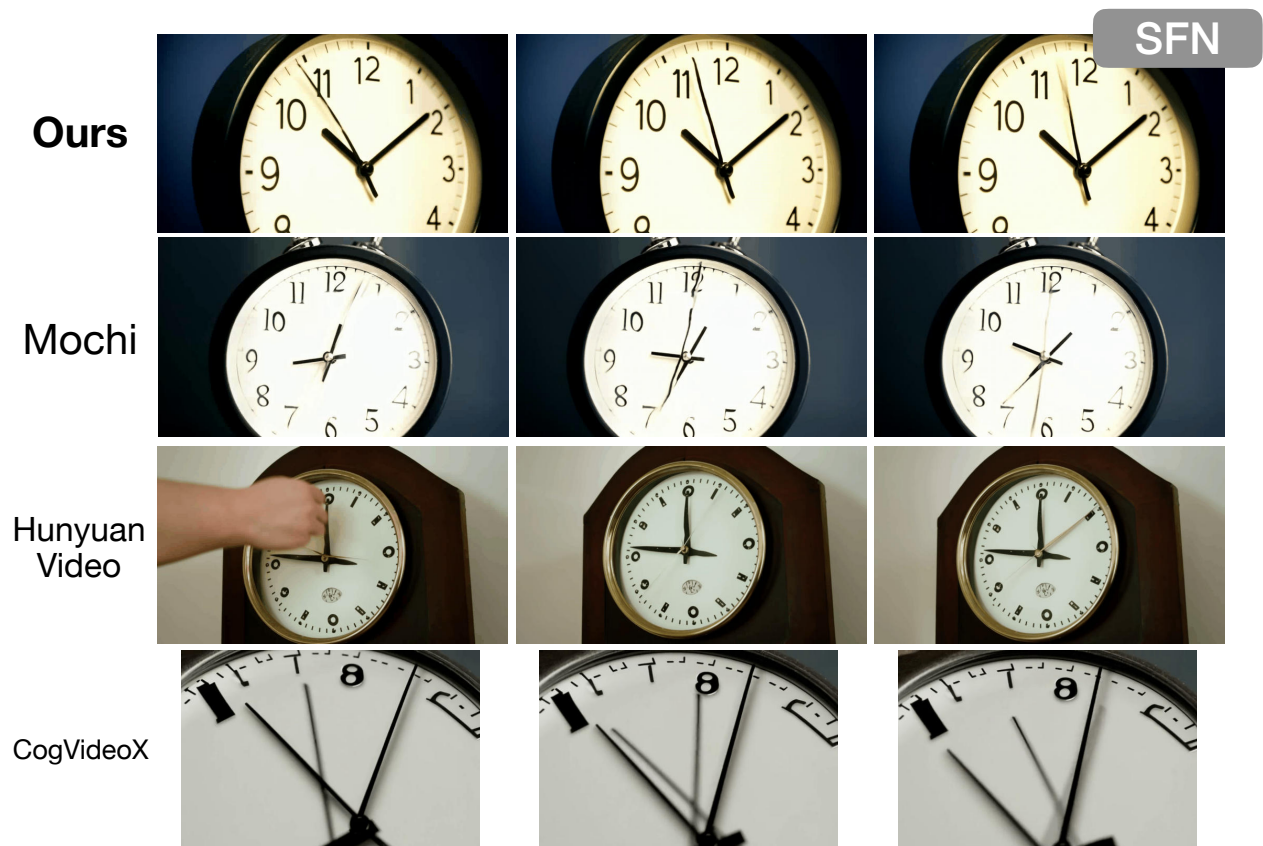
"A meadow under the night sky with **only** grass and stars."

Figure 19. **Qualitative comparison under the INA (Implicit Natural-Only Attribute) scenario.** Prompt: "A meadow under the night sky with only grass and stars." Our model preserves a purely natural scene without introducing artificial structures. Baselines frequently insert buildings or synthetic elements, demonstrating difficulty enforcing implicit natural-only constraints.



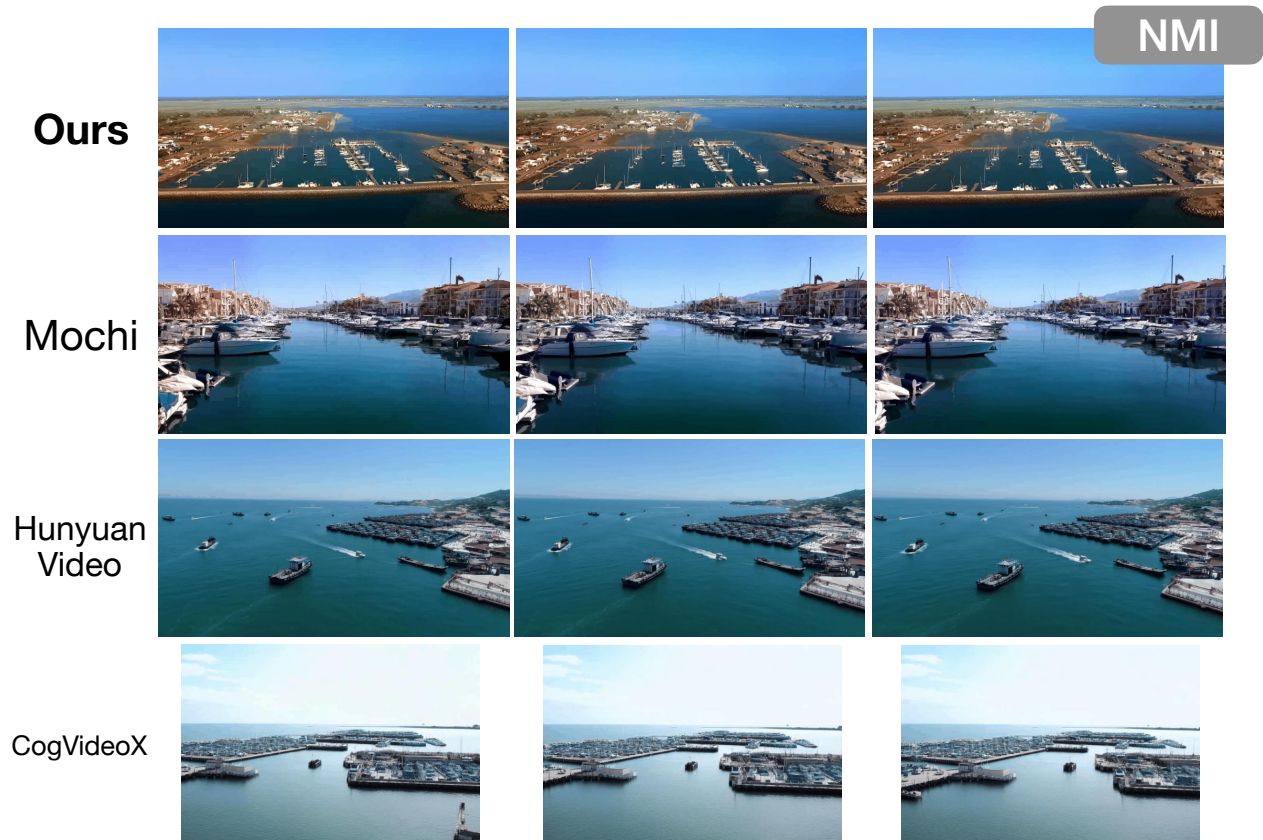
"A mountain cabin with **no** doors, **no** windows, and **no** chimney."

Figure 20. **Qualitative comparison under the MNC (Multi-Negation Composition) scenario.** Prompt: "A mountain cabin with no doors, no windows, and no chimney." Our model simultaneously enforces multiple negation constraints while preserving global structure. Competing models fail to remove all prohibited components, often leaving doors or windows visible.



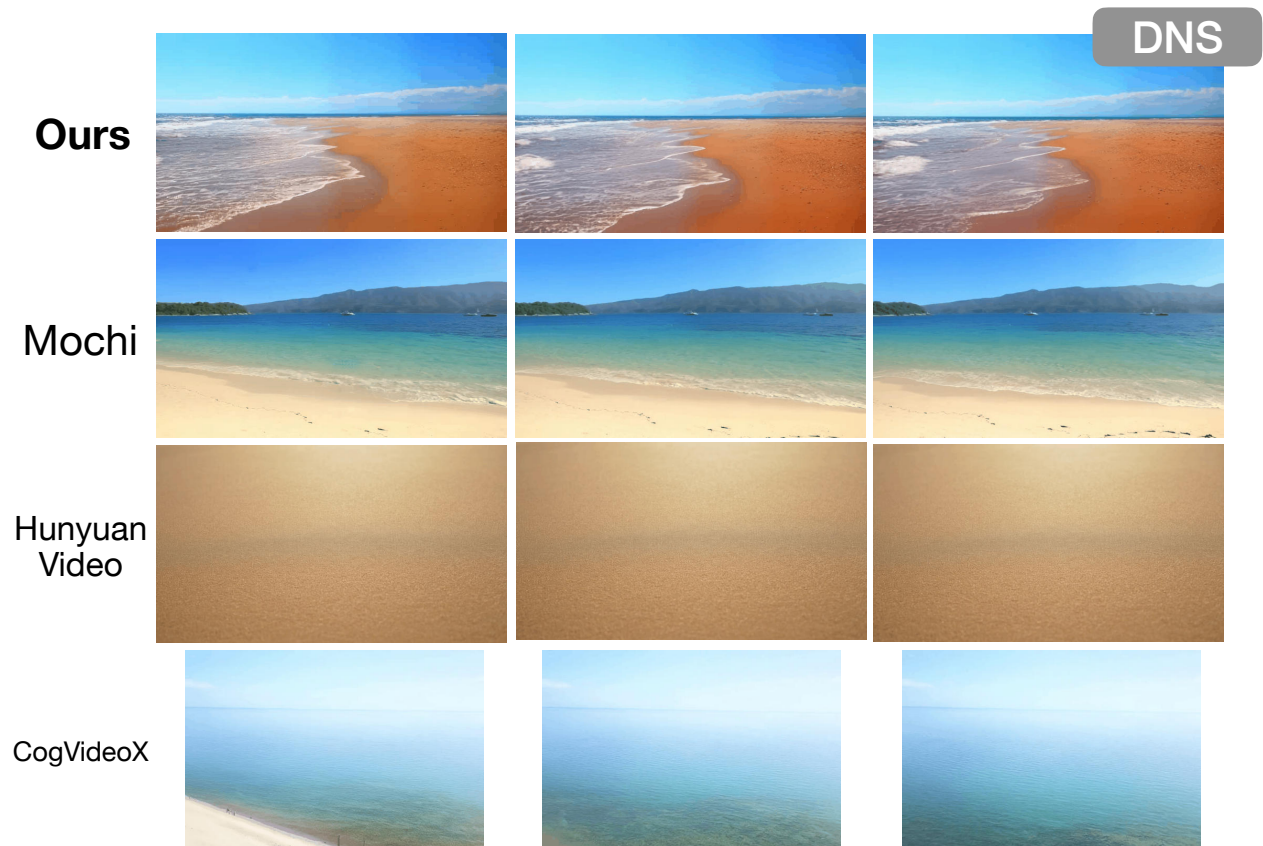
"A clock ticking but **not** moving its hands."

Figure 21. **Qualitative comparison under the SFN (Structural Functional Negation) scenario.** Prompt: "A clock ticking but not moving its hands." Our model captures the semantic distinction between object activity and functional motion. Notably, HunyuanVideo misinterprets the constraint and shows moving a person's hands, while other baselines fail to maintain consistent negation behavior.



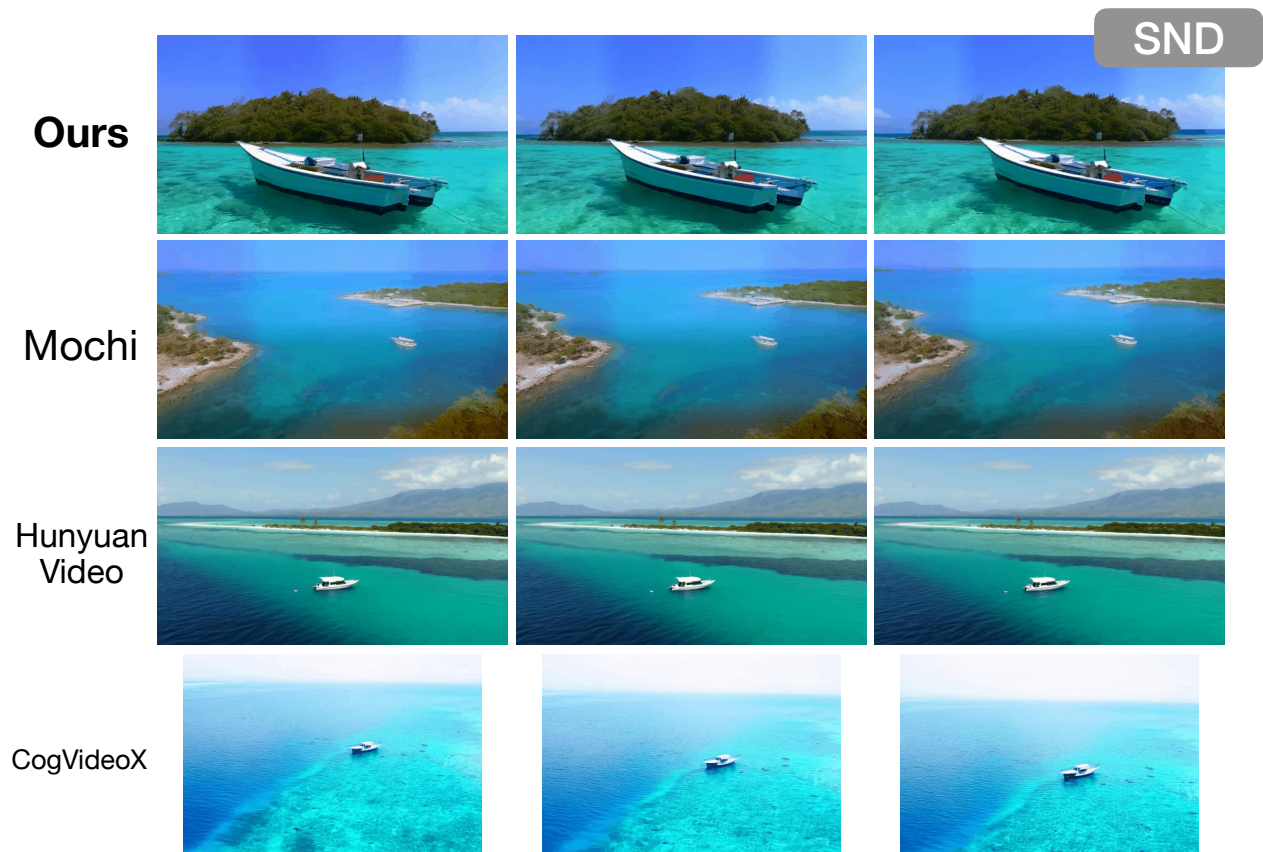
"A harbor that is *not* fully occupied."

Figure 22. **Qualitative comparison under the NMI (Negation with Moderated Intensity) scenario.** Prompt: "A harbor that is not fully occupied." Our model correctly represents partial occupancy while respecting the negation condition. Baseline methods frequently produce fully crowded scenes, indicating poor control over graded negation semantics.



*"A beach that is **not** shell-less."*

Figure 23. **Qualitative comparison under the DNS (Double Negation Sensitivity) scenario.** Prompt: "A beach that is not shell-less." Our model correctly resolves the double-negation constraint and generates beaches containing shells. Baselines often collapse to trivial empty scenes or fail to capture the intended semantic inversion.



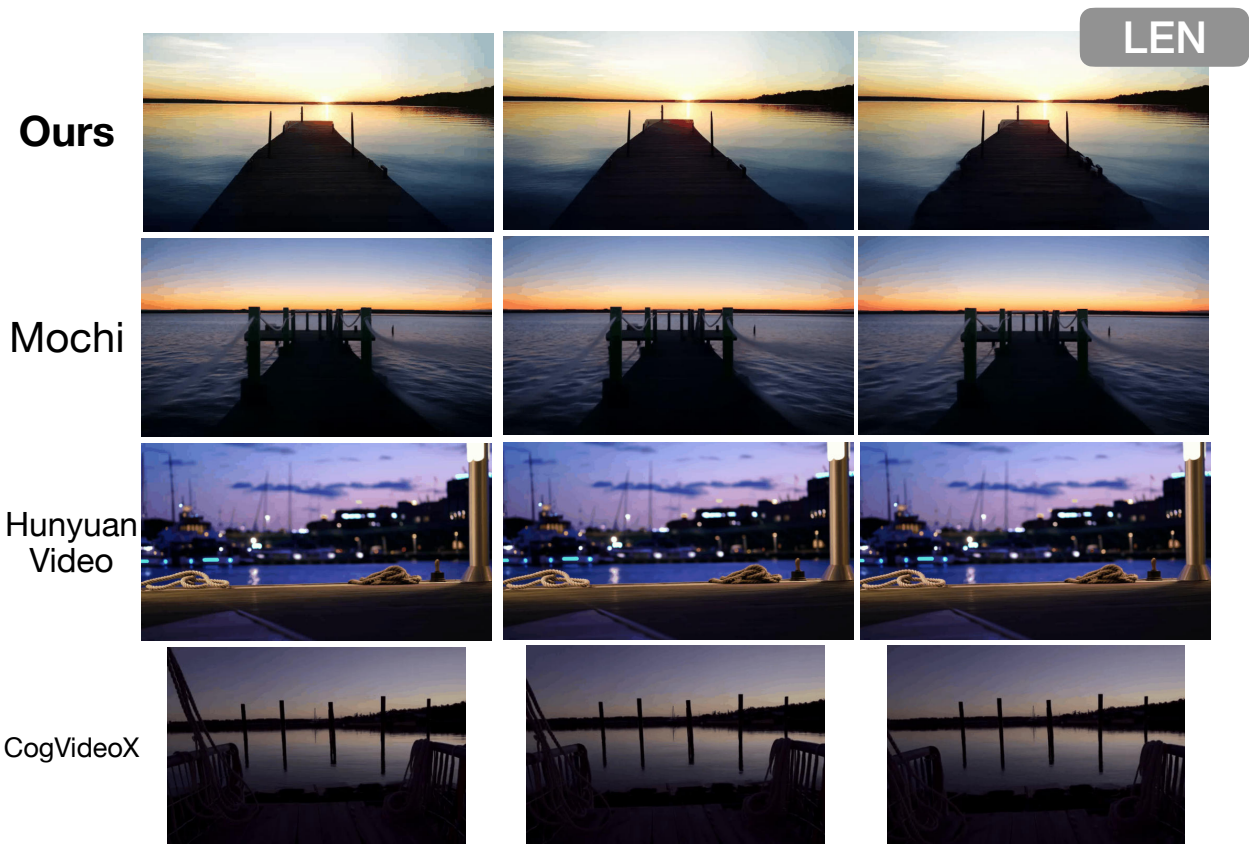
*"A boat anchored near an island that is **not** inhabited."*

Figure 24. **Qualitative comparison under the SND (Scoped Negation Disambiguation) scenario.** Prompt: "A boat anchored near an island that is not inhabited." Our model correctly applies the negation constraint to the island while preserving the boat. Competing models frequently misinterpret the scope, altering the boat or generating populated islands.



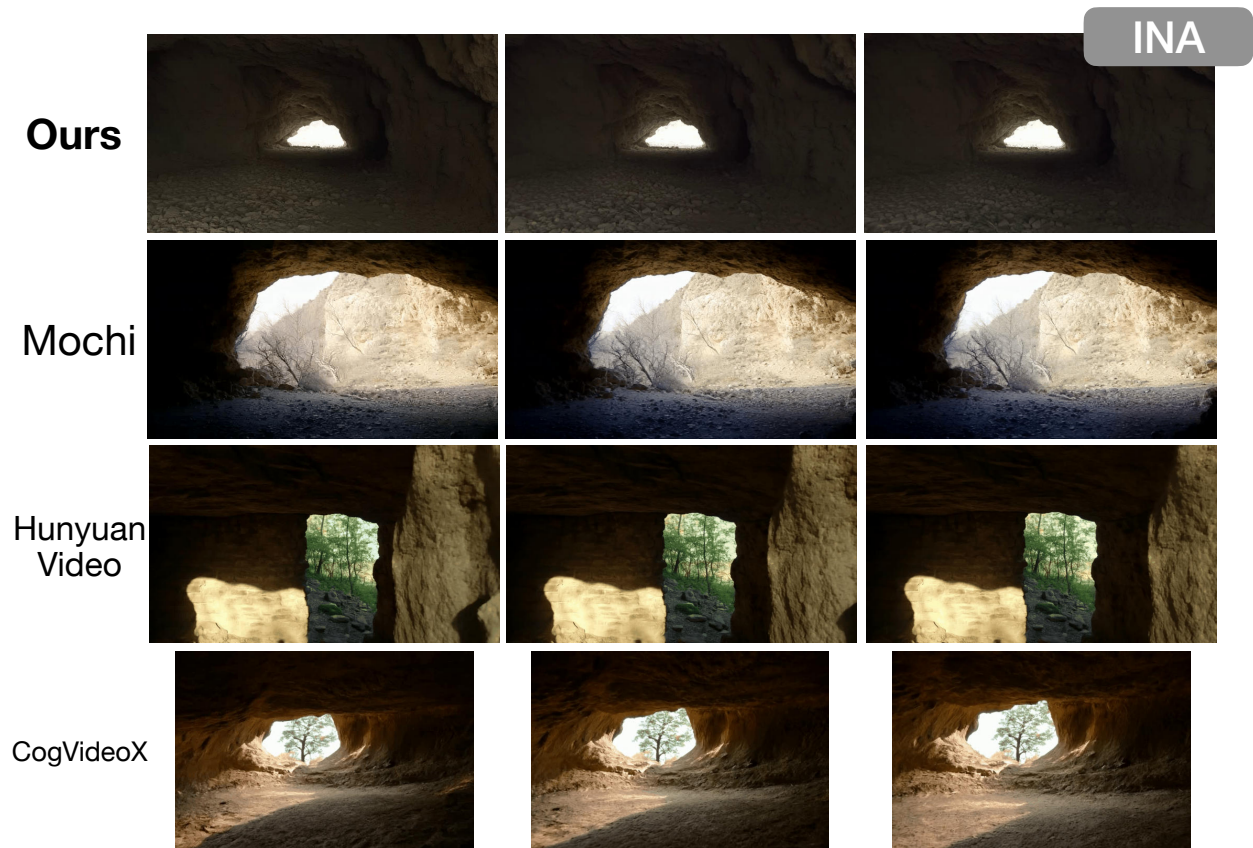
"A snowfield, with **no** footprints."

Figure 25. **Qualitative comparison under the AOC scenario.** Prompt: "A snowfield, with no footprints." Our model generates a clean untouched snowfield consistent with the negation constraint. Baseline methods frequently introduce footprints or surface artifacts.



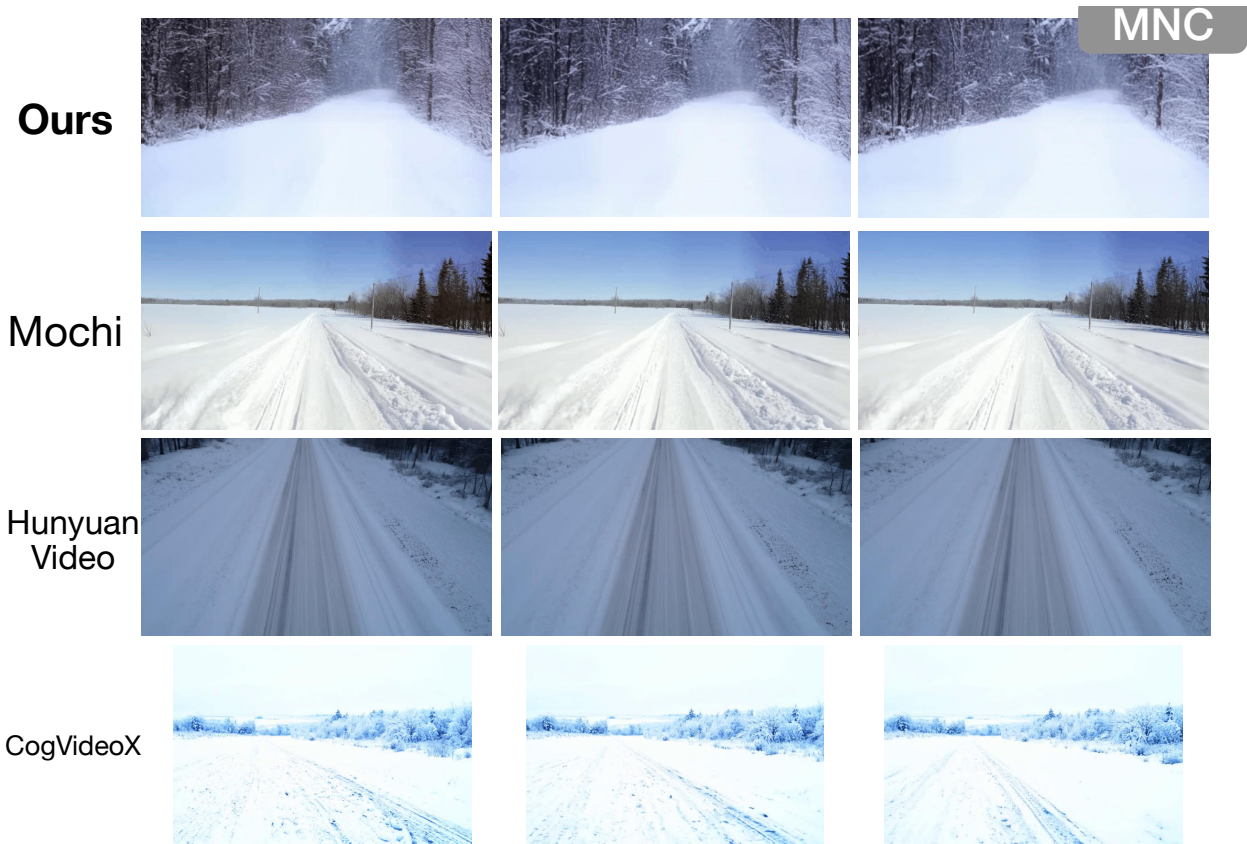
*"A dock at dusk, with **no** ropes appearing."*

Figure 26. **Qualitative comparison under the LEN scenario.** Prompt: "A dock at dusk, with no ropes appearing." Our model correctly suppresses rope structures while maintaining scene realism. Baselines often introduce ropes or structural elements violating the negation constraint.



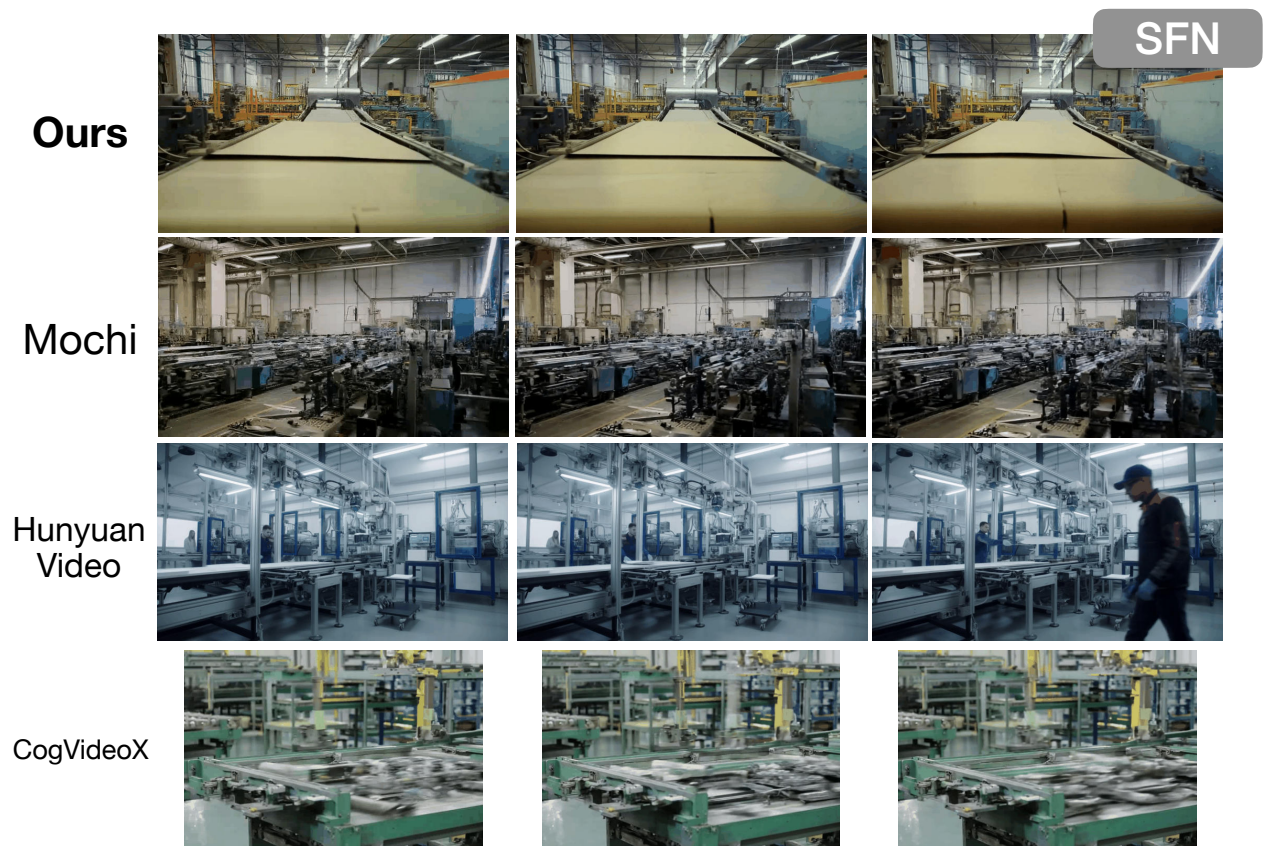
*"A natural cave interior featuring **only** stone and shadows."*

Figure 27. **Qualitative comparison under the INA scenario.** Prompt: "A natural cave interior featuring only stone and shadows." Our model maintains a purely geological environment, while competing models frequently introduce vegetation or artificial lighting elements inconsistent with the prompt.



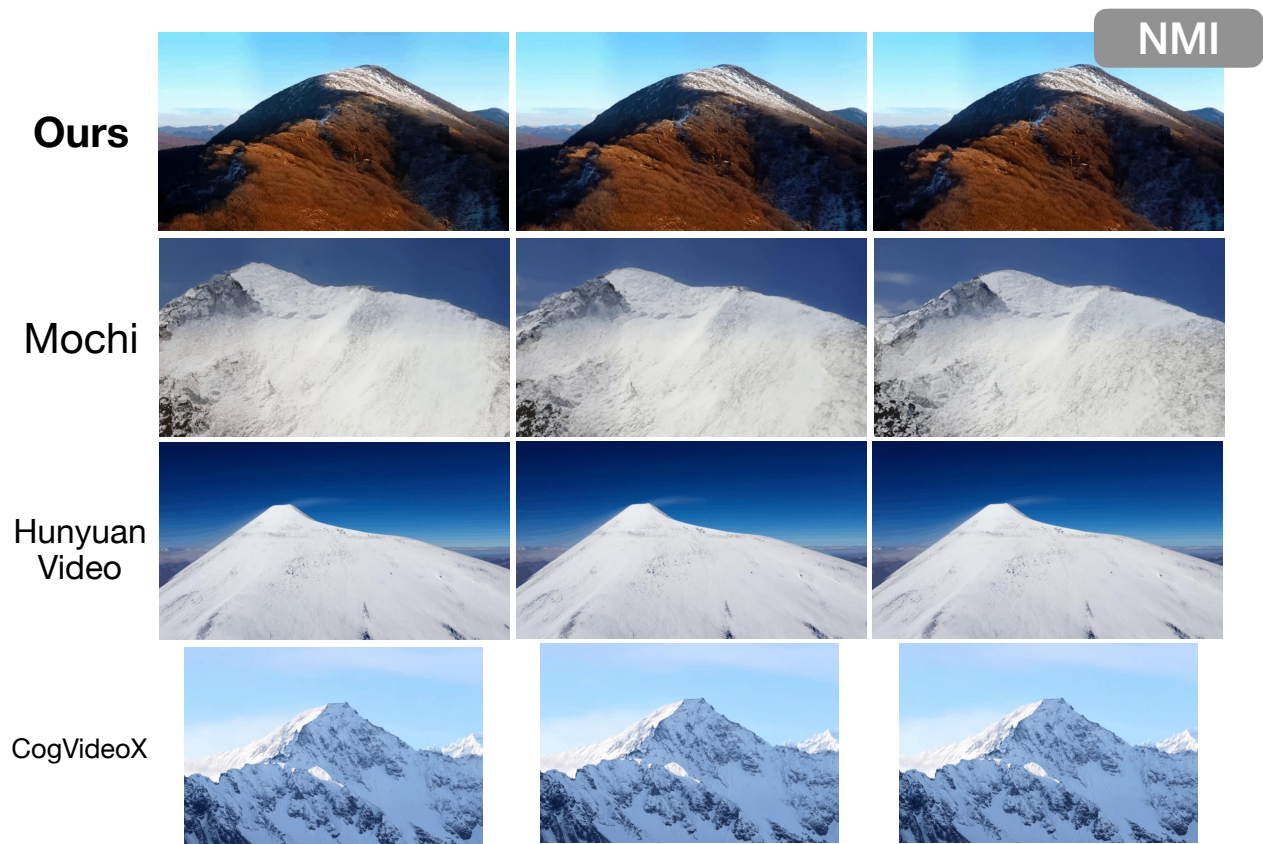
"A snow-covered road with **no** tire tracks, **no** signs, and **no** vehicles."

Figure 28. **Qualitative comparison under the MNC scenario.** Prompt: "A snow-covered road with no tire tracks, no signs, and no vehicles." Our model enforces multiple negation constraints simultaneously, producing a clean road. Baseline models commonly violate at least one constraint.



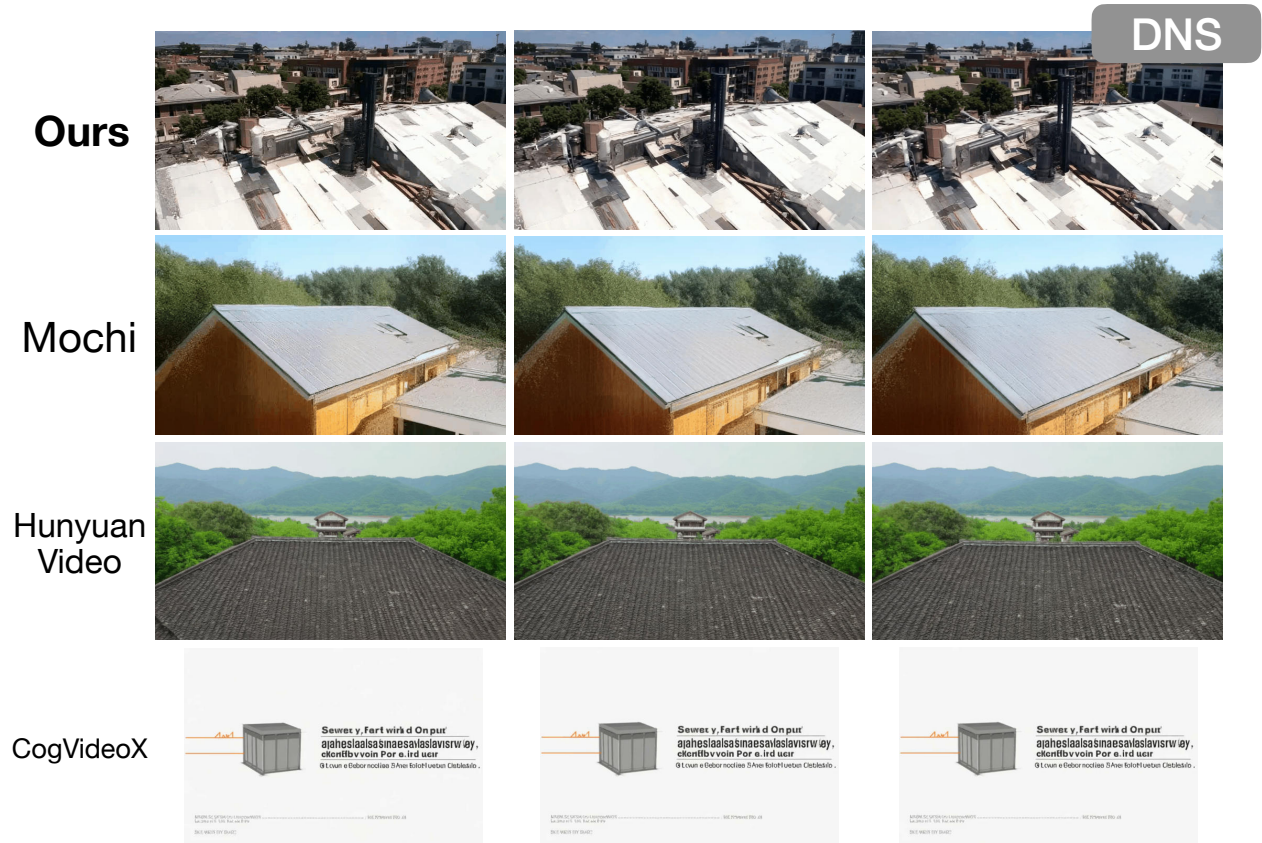
*"A factory assembly line active but **not** producing items."*

Figure 29. **Qualitative comparison under the SFN scenario.** Prompt: "A factory assembly line active but not producing items." Our model separates mechanical motion from product output, preserving activity without generated items. Baselines frequently produce items or misinterpret the constraint entirely.



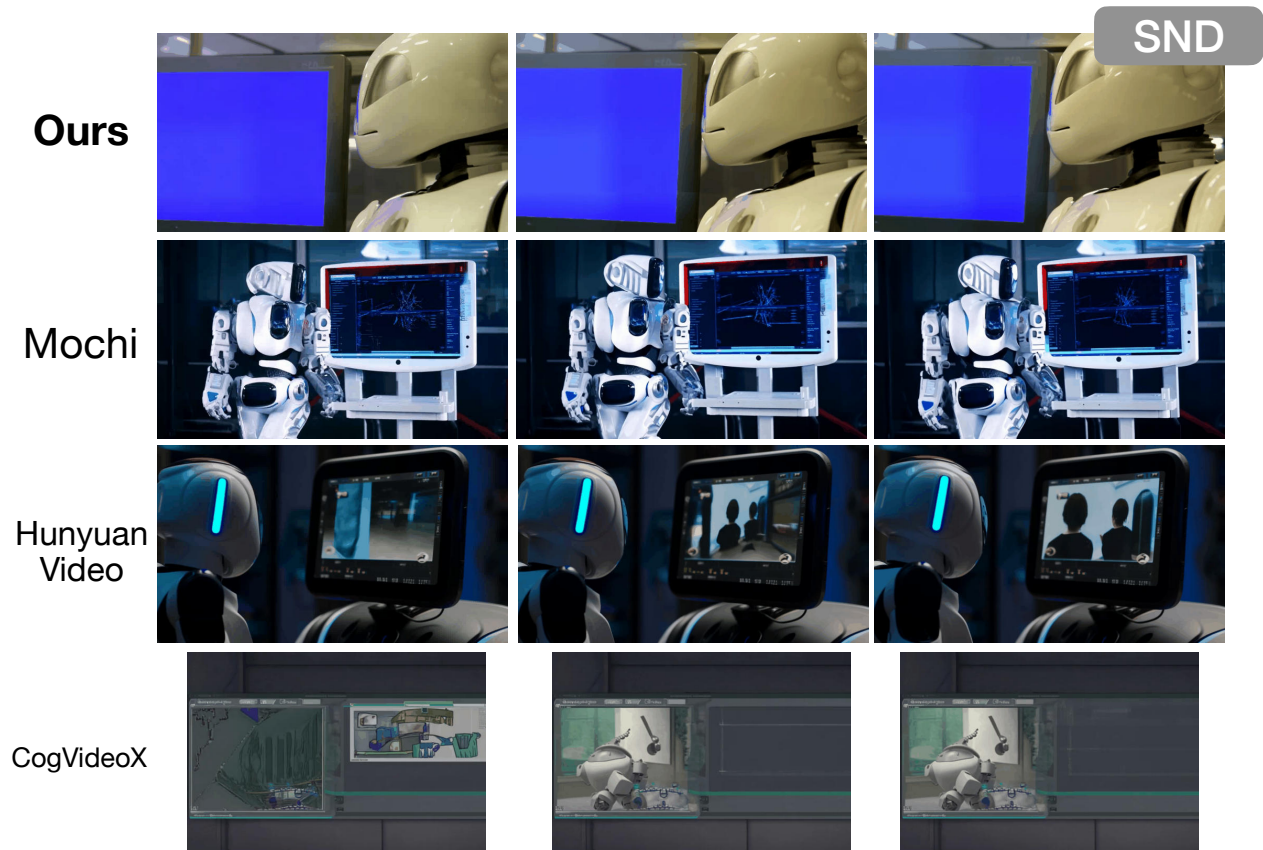
*"A mountain peak that is **not** completely snow-covered."*

Figure 30. **Qualitative comparison under the NMI scenario.** Prompt: "A mountain peak that is not completely snow-covered." Our model correctly produces partial snow coverage. Baselines often generate fully snow-covered peaks, ignoring the moderated negation constraint.



"A rooftop that is *not vent-less*."

Figure 31. **Qualitative comparison under the DNS scenario.** Prompt: "A rooftop that is not vent-less." Our model correctly resolves double negation and generates rooftops with vents. Baselines frequently ignore the constraint and produce vent-less rooftops.



"A robot next to a screen that is **not** displaying content."

Figure 32. **Qualitative comparison under the SND scenario.** Prompt: "A robot next to a screen that is not displaying content." Our model correctly applies the negation constraint to the screen while maintaining the robot and surrounding environment. Baseline methods often display content on the screen or misapply the negation to unrelated objects.